Evidence for the Relative Timing and Character of Proterozoic Deformation and Metamorphism in the Ladron Mountains, New Mexico

By

Terry Robin Pollock

B.S., University of Illinois-Urbana, 1989

THESIS

Submitted in Partial Fulfillment of the

Requirements for the Degree of

Master of Science in Geology

New Mexico Institute of Mining and Technology

Socorro, New Mexico

December, 1994

ACKNOWLEDGMENTS

I would like to thank all of my committee members: my advisor Laurel Goodwin for her continual encouragement and infinite assistance with this study, Paul Bauer for initiating the project and for many helpful discussions, and also Bill McIntosh for helping to clarify various points of this research. Much appreciation goes to Bill Chavez for use of his mineral separation laboratory and also Sam Bowring for U-Pb isotopic dating.

Many thanks to my colleagues and friends whose continual humor provided some sanity and whose advice added to improvements of this report, especially "Cos", Randy, Greg, "Reb", "The Kidd", Scottie, Ernie, and Tim "Dude".

Permission to access my field area across his ranch was kindly given by Mr. Joe Waldrum. This thesis was partially supported by funds from the New Mexico Bureau of Mines and Mineral Resources, the New Mexico Geological Society, the Anita and Antonious Budding Award, and the Geological Society of America.

Finally, inexpressible gratitude goes to my Mom and Dad for their endless love and support (both emotionally and financially) during this seemingly endless affair.

Evidence for the Relative Timing and Character of Proterozoic Deformation and Metamorphism in the Ladron Mountains, New Mexico

By

Terry Robin Pollock

ABSTRACT OF THESIS

Submitted in Partial Fulfillment of the
Requirements for the Degree of

Master of Science in Geology

New Mexico Institute of Mining and Technology
Socorro, New Mexico

December, 1994

EVIDENCE FOR THE RELATIVE TIMING AND CHARACTER OF PROTEROZOIC DEFORMATION AND METAMORPHISM IN THE LADRON MOUNTAINS, NEW MEXICO

Terry Robin Pollock

B.S. Geology, University of Illinois-Urbana, 1989

M.S. Geology, New Mexico Institute of Mining and Technology, 1994

Two main deformational events (D_1 and D_2) are recorded by the plutonic and supracrustal rocks of the Ladron Mountains. The dominant NE-striking foliation (S_2) of the study area, which records oblique-normal (west-side-up) shear, can be correlated with the dominant Proterozoic deformational fabric found throughout New Mexico. Elsewhere in New Mexico, S_2 has obliterated all but traces of the character of the older D_1 event. In the Ladron Mountains, however, D_1 is locally recorded by an E-W subvertical foliation (S_1) that preserves evidence for dextral strike-slip shear. In northern New Mexico, D_1 and D_2 were both interpreted as part of a continuous deformational event. The above mentioned relationships suggest that they were in fact distinct in character. Post-D_2 structures are locally developed and include pseudotachylyte, fractures, and open folds and crenulations in S_2. Growth of amphibole, mica, and garnet was synchronous with D_2, but metamorphism outlasted D_2. Metamorphic mineral assemblages and microstructural analyses suggest that both D_1 and D_2 were accompanied by amphibolite facies metamorphism. Locally, aligned chlorite porphyroblasts and alteration of biotite, garnet and staurolite indicate minor retrogression following peak metamorphism.

U-Pb concordia dates on igneous zircon of 1658 ± 3 Ma and 1658 ± 20 Ma for both a felsic metavolcanic rock and the (informally named) Bandit granophyre, respectively, allow for the occurrence of contemporaneous volcanism and plutonism. Intrusive and overprinting relationships suggest that the Bandit granophyre intruded pre-D_1 and the Capirote quartz monzonite intruded pre-D_2. However, both granitoids have previously been considered phases of the same pluton based on geochemical similarity. Intrusion of the Ladron quartz monzonite, whose Rb-Sr age of ~1300 Ma suggests it is probably one of the 1.4 Ga plutons found throughout the

southwest, post-dated D_2. Thus, the maximum age of D_1 is 1.66 Ga and the minimum age of D_2 is 1.4 Ga.

Detailed study of the Proterozoic rocks of the Ladron Mountains has enhanced our understanding of the Proterozoic tectonic evolution of New Mexico. Specifically, it has been demonstrated that D_1 probably occurred at ca. 1.6 Ga and involved dextral strike-slip shearing, consistent with models of Early Proterozoic crustal accretion in the southwestern United States. The timing of D_2, which produced the main NE-striking fabric throughout New Mexico and Arizona, is less clear. Within the Ladron Mountains, D_2 clearly post-dated intrusion of the Capirote quartz monzonite but pre-dated intrusion of the Ladron quartz monzonite, which is inferred to be 1.4 Ga in age. Whether D_2 is late 1.6 Ga or early 1.4 Ga in age, or somewhere in between, remains to be determined. U-Pb dating of igneous zircon in the Capirote quartz monzonite and of metamorphic sphene (that grew during D_1 and/or D_2) in the amphibolites could discriminate between these possibilities.

TABLE OF CONTENTS

LIST OF FIGURES

LIST OF TABLES

LIST OF PLATES

1. INTRODUCTION

Early Proterozoic crust of the southwestern United States was accreted to the southern margin of the Archean Wyoming province between about 1.8 and 1.6 Ga (Condie et al., 1987). The main exposures of Early Proterozoic rocks are found in a 1300-km-wide, NE-trending, orogenic belt extending from southern Wyoming to Sonora, Mexico (Karlstrom and Bowring, 1988). The details of the tectonic evolution of this belt remain controversial. One scenario, based on metavolcanic belts and metasedimentary outcrops in southern Wyoming and Colorado, involves the successive accretion of arcs and sedimentary basins to the southeast margin of the North American craton beginning at 1.77 Ga (Condie, 1982, 1986; Condie et al., 1987; Reed et al., 1987). Based on work in central Arizona, Karlstrom and Bowring (1988, 1991) suggested assembly of crustal blocks of diverse tectonostratigraphic histories during episodes of convergent tectonism at ca. 1.74-1.70 and 1.65 Ga.

Recently, attention has been focused on the character of deformation and metamorphism recorded by these accreted terranes in New Mexico. Multiple deformational and metamorphic events have affected the Proterozoic rocks. Two conflicting models of the Proterozoic tectonic history of New Mexico have been proposed. The models differ in the timing of the main deformational and metamorphic event recorded by structures and mineral assemblages. The first model, based on $^{40}Ar/^{39}Ar$ thermochronology on metamorphic minerals, places the major orogeny at ca. 1.4 Ga during widespread "anorogenic" plutonism. Both the ca. 1450 Ma Sandia pluton (Brookins and Majumdar, 1982) and 1427 Ma Priest pluton (Bauer et al., 1993) in the Sandia and southern Manzano Mountains (Fig. 1), respectively, are enveloped by contact metamorphic aureoles and are interpreted to be syntectonic with respect to deformation and associated fabric development (Thompson et al., 1991). In the southern Manzano Mountains, $^{40}Ar/^{39}Ar$ plateau ages on muscovite (1400-1420 and 1340-1360 Ma) and hornblende (1400-1440 Ma) are interpreted to reflect widespread metamorphism and plutonism at ca. 1440 Ma, long after tectonic assembly, and a subsequent thermal event at ca. 1350 Ma (Dallmeyer et al., 1990; Thompson et al., 1991). Similarly, in the Cimarron Mountains (Fig. 1), Grambling and Dallmeyer (1993) interpreted

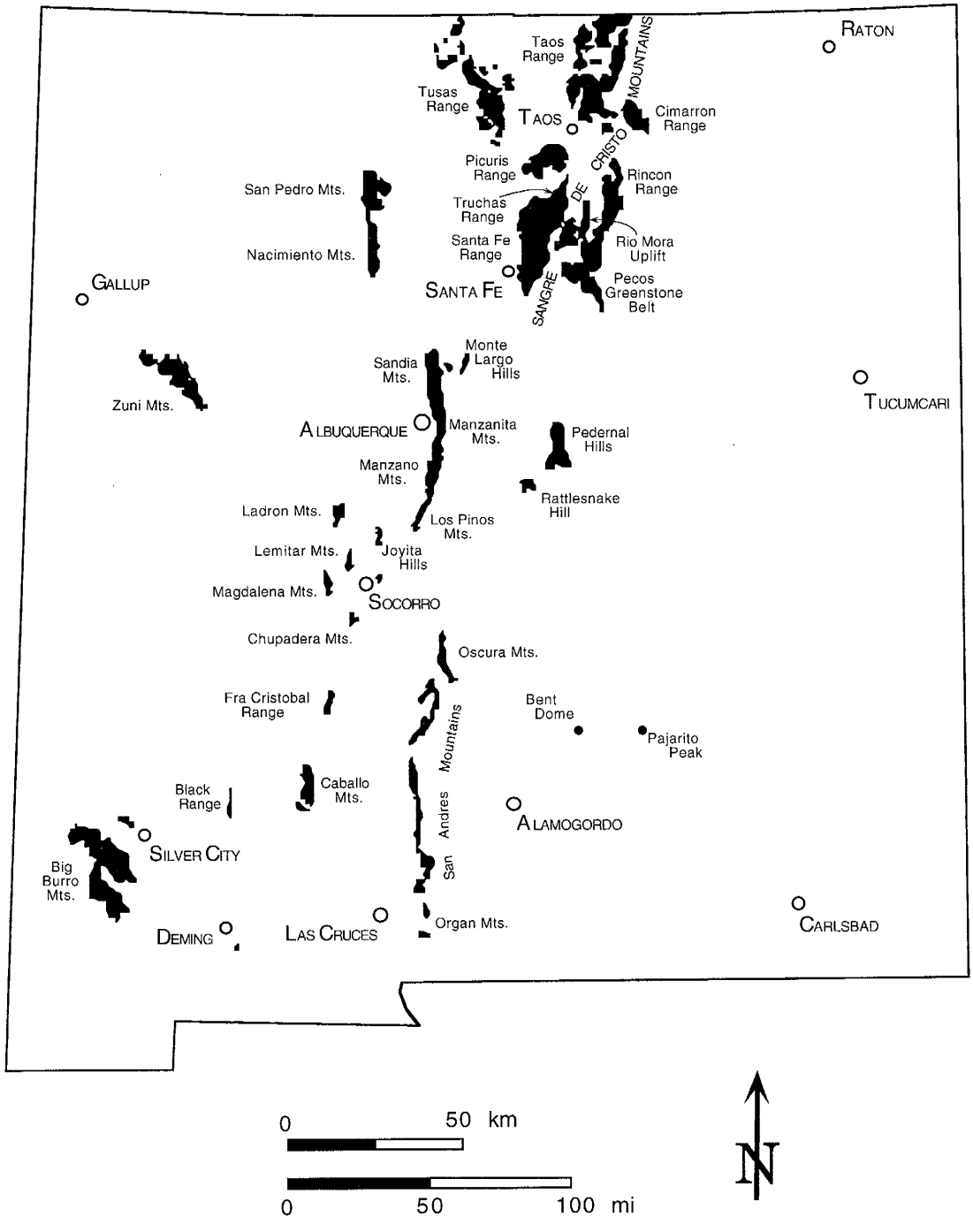

Figure 1. Map of Precambrian-cored uplifts in New Mexico (after Bauer and Pollock, 1993).

hornblende plateau ages (1394-1398 Ma) to record cooling shortly after deformation and metamorphism at ca. 1420 Ma and muscovite ages (1350, 1250, and 1100 Ma) to date subsequent thermal events. Thus, this first hypothesis states that major deformation and metamorphism occurred around 1.4 Ga.

The second model is supported by field-based structural analyses, metamorphic studies, and U-Pb crystallization dates on undeformed and strongly deformed plutonic and volcanic rocks. Bowring and Karlstrom (1990) suggested that major deformation and prograde metamorphism accompanied tectonic assembly and magmatism at 1.65-1.66 Ga in southeastern Arizona during the Mazatzal orogeny. This orogenic event has been interpreted to also include the multiply deformed Proterozoic rocks of central and northern New Mexico (Williams, 1990). In several areas the strongly deformed granitoids and associated supracrustal rocks are older than 1.6 Ga, whereas granitoids associated with the 1.4 Ga plutonic event are only weakly deformed (Bowring et al., 1983; Bauer et al., 1993). A unique case in which the age of major deformation can be tightly constrained is in the Magdalena Mountains (Fig. 1) where an undeformed 1654 Ma granite crosscuts the foliation in highly deformed and metamorphosed supracrustal rocks dated at 1664 Ma (Bauer and Williams, 1994). To the east of the Magdalena Mountains, in the southern Manzano Mountains, the highly sheared Monte Largo pluton is dated at 1656 Ma (Bauer et al., 1993), and the weakly foliated Priest pluton (Goodwin et al., 1992) is dated at 1427 Ma (Bauer et al., 1993). Similarly, to the north in the Picuris Mountains, the ca. 1680 Ma Rana and Puntiagudo plutons contain strong tectonic foliations whereas the ca. 1450 Ma Peñasco pluton contains a weak magmatic foliation (Bell, 1985; Bauer, 1993) (Fig.1). Other examples of 1.65-1.66 Ga strongly deformed rocks in central New Mexico include granites in the Lemitar, Chupadera, Zuni, and Los Pinos Mountains (Bowring and Condie, 1982; Bowring et al., 1983; Shastri, 1993) (Fig.1) , and metarhyolitic rocks in the Zuni and Los Pinos Mountains (Bowring and Condie, 1982; Shastri, 1993). Thus, according to this second model, the major orogeny occurred at 1.6 Ga in Arizona and New Mexico.

In the Manzano Mountains the regional foliation clearly pre-dates intrusion of the 1427 Ma Priest pluton, yet inclusion trails within contact-

metamorphic minerals are perpendicular to this foliation. This is interpreted to indicate that strain associated with pluton emplacement locally enhanced the previously developed fabric (Thompson and Karlstrom, 1993). Karlstrom and Grambling (1993) have suggested that the contribution of deformation associated with intrusion of the ca. 1.4 Ga plutons throughout New Mexico may have been overestimated by previous workers, and that emplacement locally reactivated an earlier formed (ca. 1.6 Ga) foliation within their contact metamorphic aureoles.

Furthermore, post-1.4 Ga low temperature deformation is well documented in several areas, including the Tusas (Williams, 1991), Picuris (Bauer, 1993), Cimarron (Grambling and Dallmeyer, 1993) and Manzano (Thompson et al., 1991; Goodwin et al., 1992) Mountains (Fig. 1). Williams (1991) described a late, spaced crenulation cleavage and associated upright, open folds, and Bauer (1992) documented both late brittle (vertical fractures and quartz veins) and ductile (broad folds and crenulation cleavages) structures. Fold hinges and fractures in these two areas trend roughly N-S. In the Manzano Mountains, a locally developed, post-intrusive, NE-striking mylonitic fabric has been noted in the 1427 Ma Priest pluton and its contact aureole (Goodwin et al., 1992).

The different interpretations of the relative timing of Proterozoic deformation, metamorphism, and plutonism in New Mexico may simply reflect heterogeneous strain or may result from the application of using Ar-Ar vs. U-Pb dating techniques. The first method uses metamorphic minerals to date the time of cooling through their specific blocking temperatures with respect to closure of the Ar isotopic system. Therefore, subsequent thermal event(s) which involved temperatures in excess of the blocking temperature of the specific mineral used will reset the Ar-Ar system. This usually results in Ar loss which yields a date that is younger than the age of mineral growth. The second method uses igneous zircon to date the time of crystallization, the temperature at which zircon becomes closed to the U-Pb isotopic system. Because of the high blocking temperature of zircon, U-Pb systematics usually remain closed to subsequent regional thermal events. This method can therefore be used to date the age of crystallization even after the rocks experience metamorphism. The lack of studies which combine both dating methods in

a single area also leads to different interpretations of the relative (and absolute) timing of events.

This investigation of Proterozoic metamorphic and plutonic rocks of the Ladron Mountains had two major goals: (1) to expand the areas of detailed structural studies in New Mexico; and (2) to evaluate the previously proposed tectonic models. The Ladron Mountains were chosen for this study because they include 1.6 and 1.4 Ga granitoids which intrude metamorphic rocks with appropriate lithologies for interpreting metamorphic grade. Detailed structural, metamorphic, and geochronologic studies have been used to establish the Proterozoic geologic history. Specific points that have been addressed include: 1) the relative timing of deformation, metamorphism, and intrusion; 2) metamorphic grade and sense of shear during different deformational events; and 3) the absolute ages of plutonic and metavolcanic rocks.

2. GEOGRAPHY, GEOLOGY, AND METHODOLOGY

2.1 ACCESS AND GEOGRAPHY

The Ladron Mountains are located in central New Mexico, 50 km northwest of Socorro (Figs. 1 and 2). The easiest access to the area is from I-25 at the Bernardo exit (Fig. 2). A well-kept dirt road leads northwest through the Sevilleta National Wildlife Refuge onto ranchlands. A secondary road off the main road continues to the east flank (Fig. 2). This road ends at the Waldrum Ranch, from which point it is necessary to hike into the main east-west drainage (Fig. 3).

The mountains are characterized by moderately to extremely rugged terrain with about 1000 m of relief. Vegetation ranges from abundant scrub juniper and cactus to grasses and pines depending on elevation. Exposure ranges from about 20% at lower elevations to 80% on the high, steep ridges.

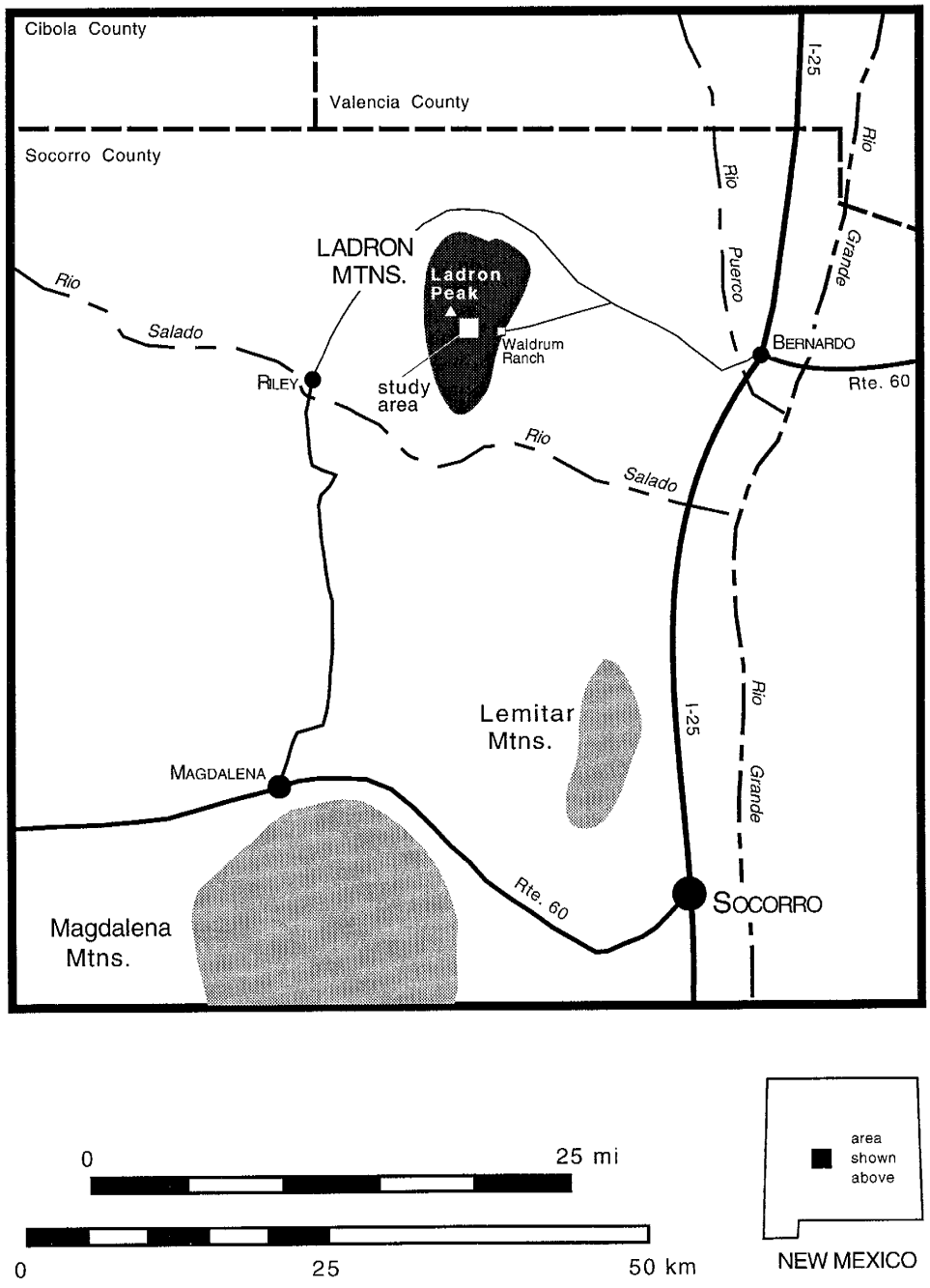

Figure 2. Location and access of study area (after Taylor, 1986).

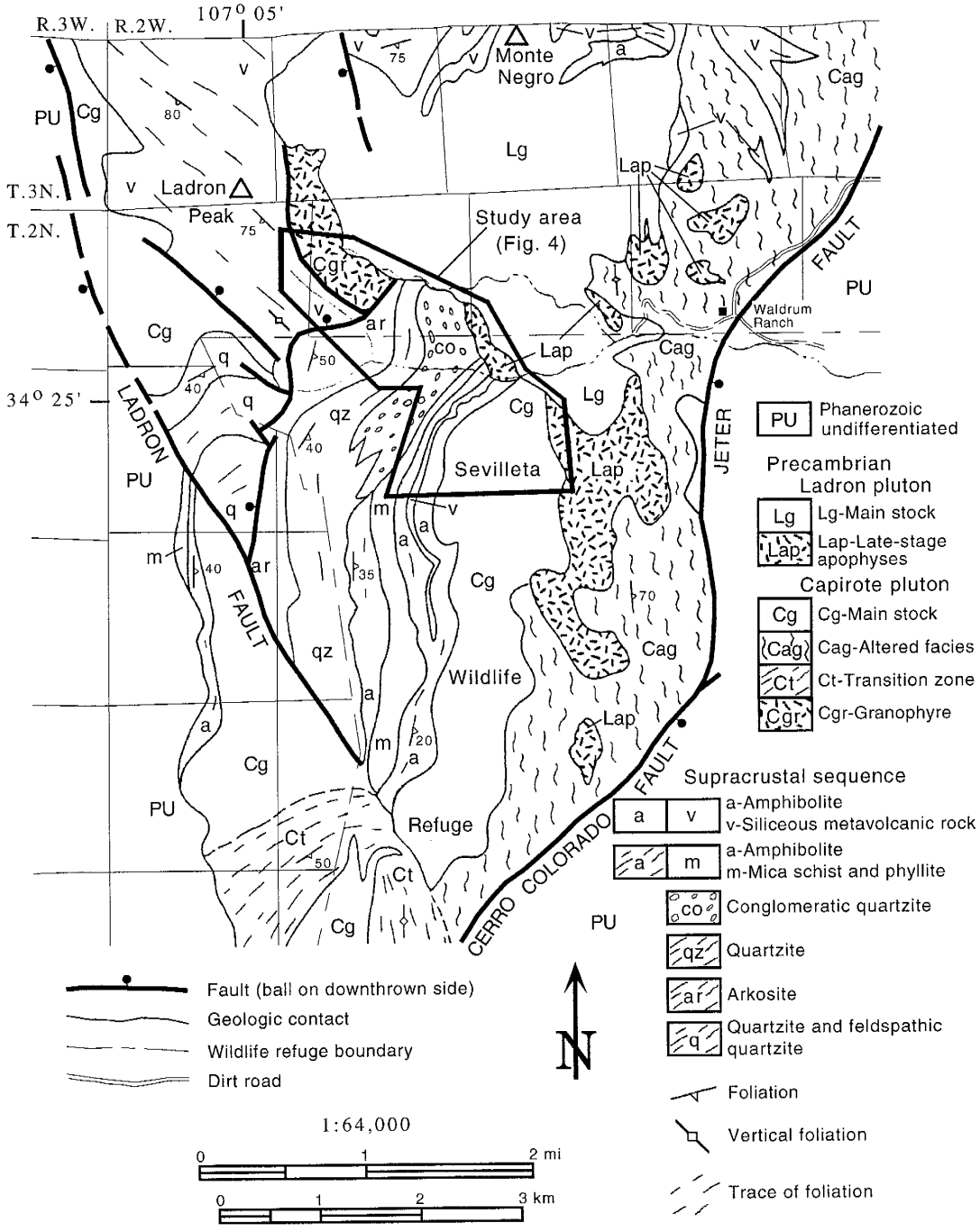

Figure 3. Geologic map of the Ladron Mountains modified from Condie (1976) and Condie and Budding (1979). Study area outlined is shown in Fig. 4.

2.2 GEOLOGIC SETTING

The Ladron Mountains are one of the few large, fault-bounded, Neogene-age uplifts that border the Cenozoic Rio Grande rift on its western edge. This Proterozoic-cored block lies near the boundary between the Colorado Plateau and Southern Rocky Mountains. Proterozoic metamorphic and plutonic rocks dominate the uplift, with minor Phanerozoic strata in fault contact with and unconformably overlying the lower western flank (Fig. 3). The western margin of the Ladron uplift is delineated by the west-dipping, high-angle normal Ladron fault, which brings into contact west-dipping Pennsylvanian strata with Proterozoic rocks (Condie, 1976). Along the eastern flank, the Jeter and Cerro Colorado faults border the Rio Grande rift. Both are normal, east-dipping faults that mark the contact between Proterozoic rocks and the younger west-dipping strata to the east (Condie, 1976) (Fig. 3). The north-striking Pennsylvanian strata on either side of the uplift, on average, dip 30° W (Noble, 1950).

2.3 PREVIOUS WORK

Previous workers have mapped lithologic contacts (Noble, 1950; Black, 1964; Condie, 1976; Taylor, 1986), completed petrographic studies of different lithologies (Haederle, 1966; Farquhar, 1976; Condie, 1976; White, 1977; Cookro, 1978; Taylor, 1986), evaluated protoliths to the metasedimentary rocks (Taylor, 1986), and attempted structural analyses (Black, 1964; Condie, 1976; Taylor, 1986) of Proterozoic rocks in the Ladron Mountains. Salient points of this previous research are summarized in the following sections.

2.3.1 **Stratigraphy**

The Proterozoic rocks in the area studied include metamorphosed supracrustal rocks and four intrusive bodies, shown on the generalized geologic map and schematic stratigraphic column (Figs. 4 and 5). Condie's (1976) classification of rock types has been used here with minor modifications. Detailed descriptions can be found in Condie (1976), Cookro (1978), and Taylor (1986). Metamorphosed clastic sedimentary and felsic

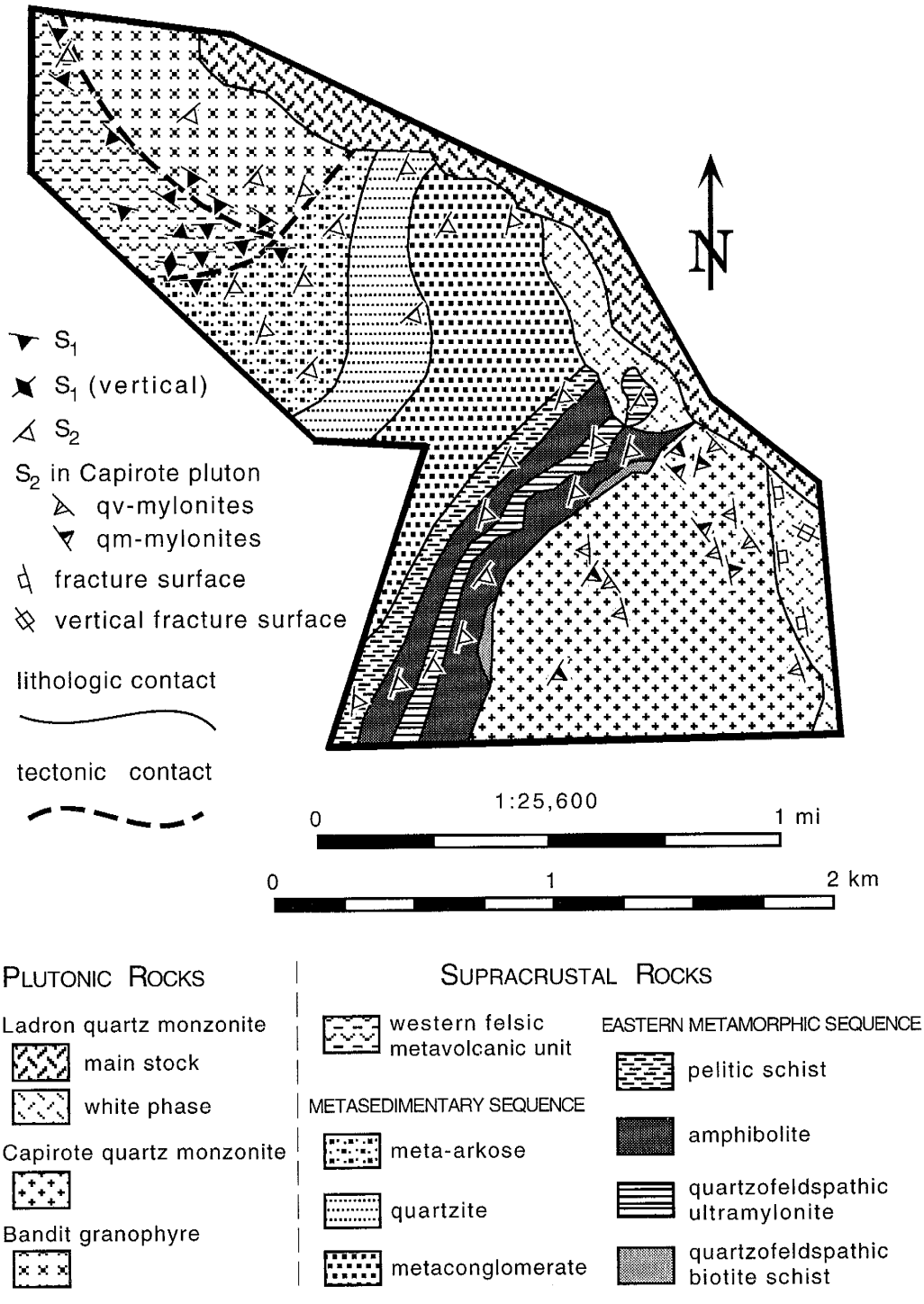

Figure 4. Generalized geologic map of the study area. Detailed structural map included in Plate 1.

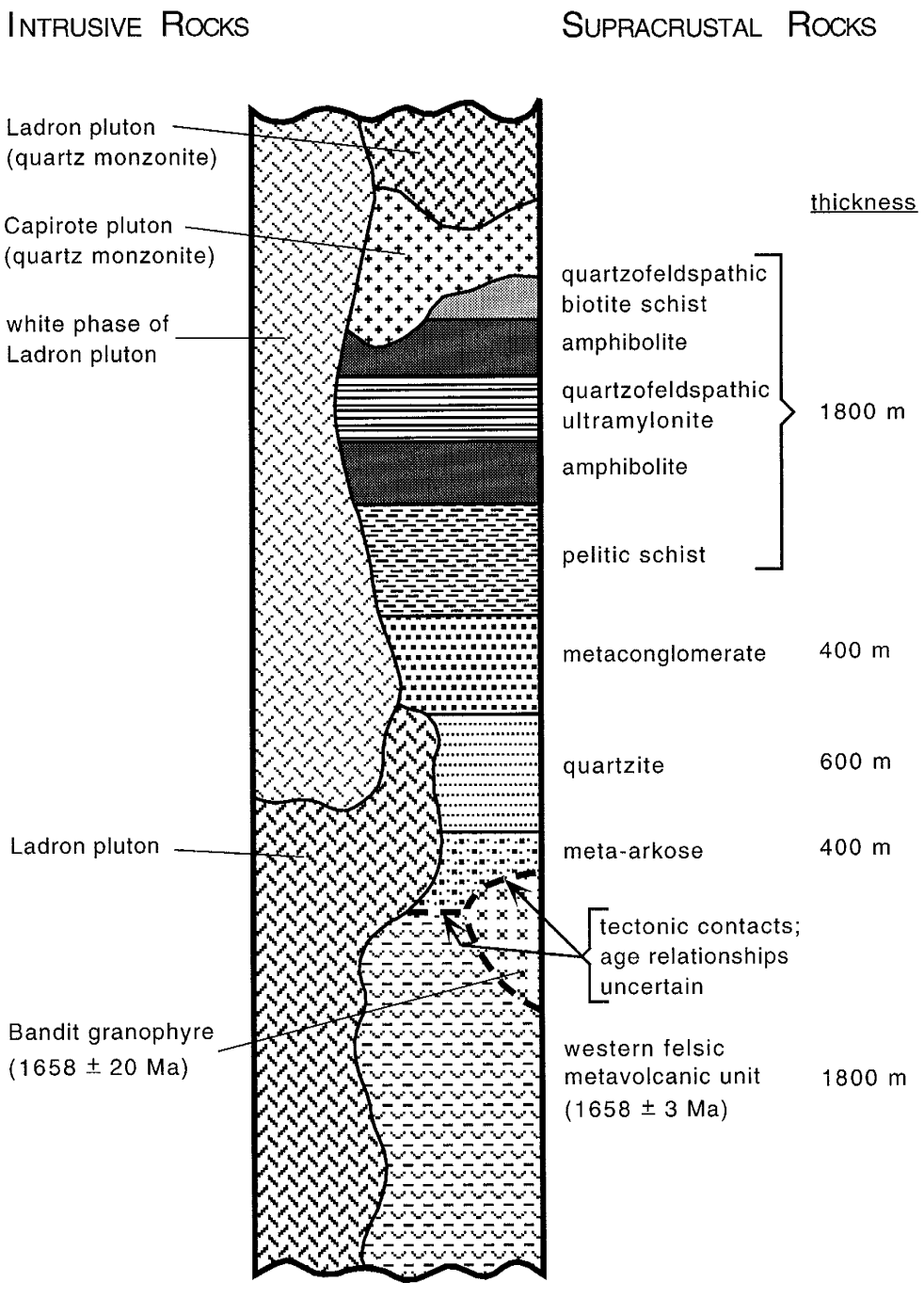

Figure 5. Schematic diagram of stratigraphy and intrusive relationships. Absolute ages of the supracrustal rocks decrease from bottom to top, except where indicated. Thicknesses from Condie (1976).

and mafic volcanic rocks constitute the metamorphic suite. A felsic metavolcanic unit in the far western part of the area contains relict phenocrysts of feldspar in an extremely fine-grained matrix. It is in contact with the meta-arkose, but the age of the metavolcanic rock relative to the rest of the sequence is unknown. Meta-arkose, quartzite, and metaconglomerate make up the stratigraphic succession from oldest to youngest (west to east) in the metasedimentary rocks as concluded from relict crossbeds and graded beds (Condie, 1976; Taylor, 1986). Lenses of pelitic schist and amphibolite are found within the metasedimentary sequence. In contact with these sediments to the east is a rock sequence (eastern metamorphic sequence; Fig. 4) interpreted to be metavolcanic (Condie, 1976; Taylor, 1986), which from bottom to top includes pelitic schist, amphibolite, quartzofeldspathic ultramylonite, amphibolite, and quartzo-feldspathic biotite schist. All exposed contacts within the metasedimentary and eastern metamorphic sequences are gradational in character (Condie, 1976; Taylor, 1986). The eastern metamorphic sequence stratigraphically overlies the metasedimentary rocks (Fig. 5). Intrusive into this supracrustal sequence are three plutons: the Capirote quartz monzonite, the Ladron quartz monzonite, and a white phase of the Ladron quartz monzonite (Fig. 5). Intrusive relationships remain unclear for a fourth pluton, the Bandit granophyre. This is a fine- to medium-grained quartz monzonite (Cookro, 1978), which contains local occurrences of anhedral garnet partially replaced by epidote.

The Capirote pluton is a medium- to coarse-grained, two-mica (biotite>muscovite) granitoid locally cut by quartz veins. The Capirote pluton intrudes both the amphibolite and quartzofeldspathic biotite schist as illustrated by a chilled margin. East of the study area, Condie (1976), Cookro (1978), and Taylor (1986) identified a transitional facies of the Capirote pluton with abundant metamorphic inclusions, indicating that it intruded following metamorphism of the metasedimentary and metamorphic sequences. Based on geochemical similarity, Cookro (1978) and Condie (1978) tentatively interpreted the Bandit granophyre as a high-level, late-stage phase of the Capirote pluton. However, Condie (1976) suggested that the granophyre is "...a fragment of a sill or shallow pluton associated with the [felsic] metavolcanic [unit]...".

The Ladron pluton is generally a coarse-grained, two-mica (muscovite>biotite) granitoid. Late stage apophyses of the Ladron granitoid are white with local occurrences of abundant muscovite and garnet (Condie, 1976). Both phases of the Ladron pluton show intrusive relationships with all surrounding units. The main pluton has chilled margins at its contact with the metasedimentary sequence. A dike of the white phase of the Ladron pluton intrudes, and contains a xenolith of, the Bandit granophyre (Fig. 6).

2.3.2 **Structure**

Condie (1976) mapped the dominant NE-striking, SE-dipping, foliation, which he interpreted as bedding-parallel, in the study area. Taylor (1986) attempted to correlate fabrics in the Proterozoic rocks with distinct deformational events. Taylor (1986) recognized two distinct episodes of deformation, which he designated D_1 and D_2. His interpretation of D_1 and D_2 fabrics was based upon numerous foliation and fold data. The bedding-parallel foliation surfaces Condie (1976) mapped and NE-trending extension lineations were interpreted to have formed by reverse shear (SE-side-up) during D_1. This shear zone model for D_1 included an increasing strain gradient from west to east, based on folds, mylonite zones, and sigmoidal clasts, all restricted to the far eastern part of the area. D_2 structures included NE- and NNW-striking conjugate cleavages and SE-plunging folds in the supracrustal rocks. The NNW-striking cleavage was not recognized in this study.

2.3.3 **Metamorphism**

Grambling (1986) concluded from garnet-biotite-plagioclase thermo-barometry that peak metamorphism occurred at 500-550° C and 3.5-4.6 kb throughout much of northern and central New Mexico. Taylor (1986) obtained electron microprobe chemical data on several garnet and biotite grains on one sample of pelitic schist from the Ladron Mountains. Profiles of major cations across garnet grains showed normal chemical zoning, indicative of prograde reactions, surrounded by a narrow band of reverse zoning suggesting retrograde reactions (Taylor, 1986). Garnet-biotite temperature calculations, based on compositions of garnet cores and biotite

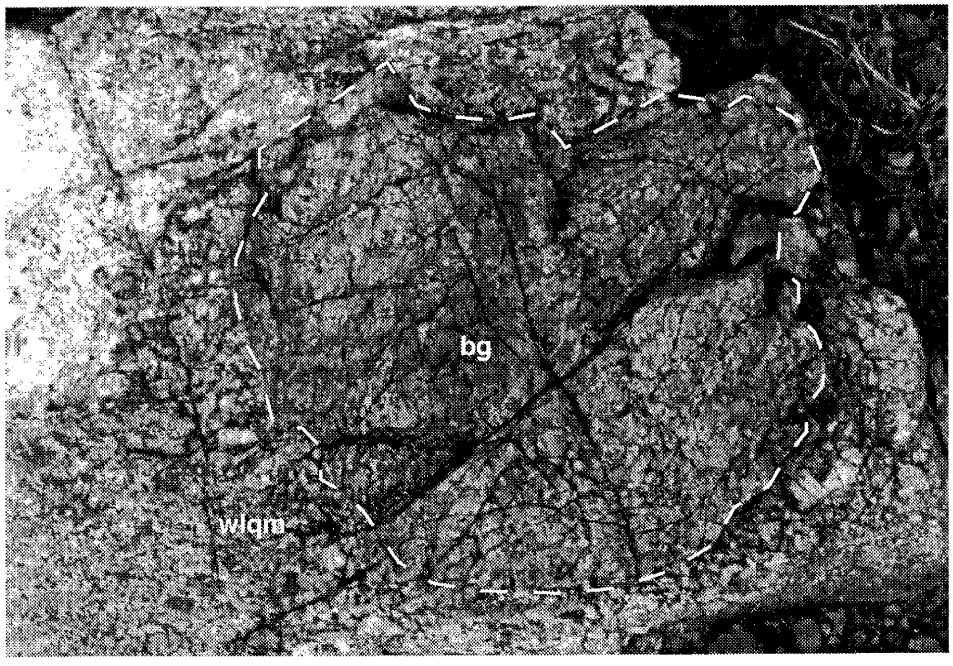

Figure 6. Intrusive relationship between the white phase Ladron pluton (wlqm) and the Bandit granophyre (bg). A xenolith of bg in a dike of wlqm. 2 m across.

grains showing minimal alteration ranged from 494° to 517° C. Pressures were estimated between 2 and 4 kb based on the coexistence of andalusite and staurolite. Andalusite requires pressures less than about 3.8 kb using the alumino-silicate phase stabilities of Holdaway (1971), whereas staurolite is usually not stable below pressures near 2 kb (Turner, 1981). Taylor (1986) also concluded from sericitization of staurolite and andalusite and reverse zoning in garnet rims that retrogression followed peak metamorphism.

Microscopic investigations undertaken for this study are included here for completeness and because they are consistent with Taylor's (1986) results. The assemblages (1) quartz + muscovite + plagioclase ± biotite ± garnet ± staurolite for pelitic schist, and (2) plagioclase + blue-green amphibole + epidote + quartz in the amphibolites are characteristic of amphibolite facies metamorphism. The appearance of chlorite replacing garnet and biotite (Fig. 7a), and sericitization of staurolite (Fig. 7b), suggests subsequent alteration or local retrogression.

2.3.4 **Geochronology**

Geochronologic investigations have been carried out on the igneous rocks in the Ladron Mountains (White, 1977). Whole-rock, Rb-Sr isotopic dates on the Ladron pluton, Capirote pluton, and felsic metavolcanic unit are 1291 ± 51, 986 ± 29, and 1143 ± 56 Ma respectively. The date for the Capirote pluton will not be considered here because it is a two point isochron. Rb-Sr isotopic systematics are commonly reset during metamorphism (Bowring et al., 1983), and thus, the date on the felsic metavolcanic unit may indicate a later thermal event at ~1150 Ma because subsequent U-Pb dating of zircon in this study gave a substantially older age of crystallization. The 1.3 Ga age on the Ladron pluton may record partial re-setting by a younger thermal event if the pluton is interpreted to have been emplaced during widespread 1.4 Ga plutonism.

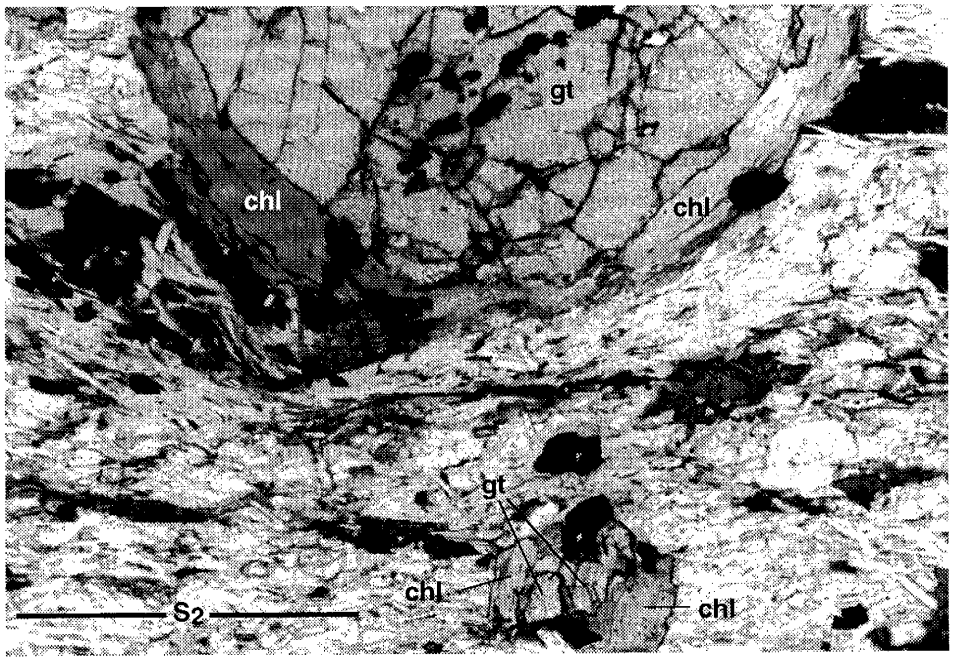

A. Large garnet (gt) porphyroblast and smaller garnet grain overgrow the foliation and and have alteration rims of chlorite (chl). Plane-polarized light; 1.6 mm across.

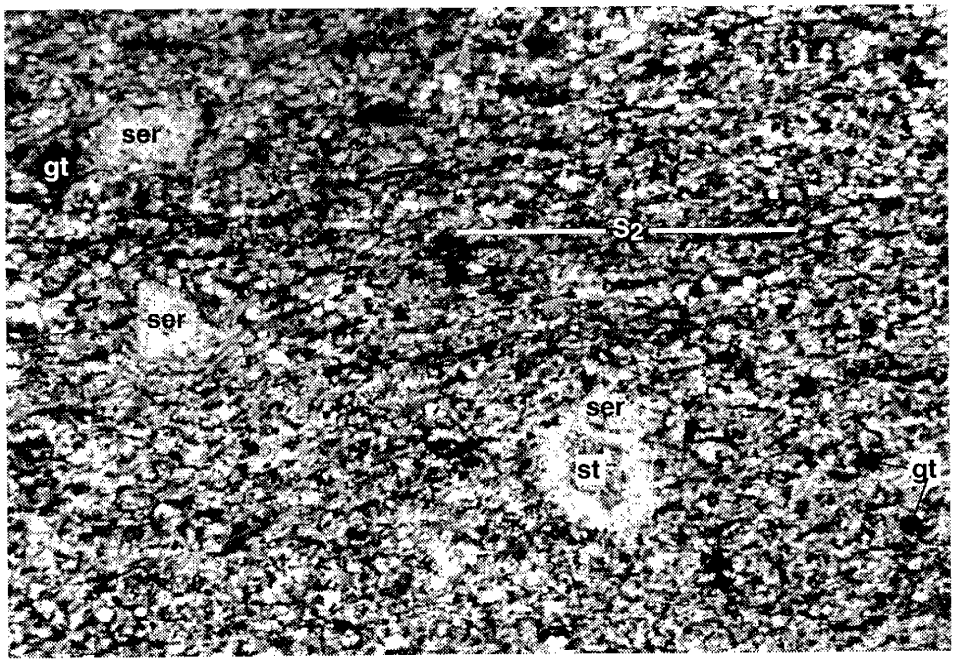

B. Relic staurolite (st) grain rimmed by sericite (ser) suggests that sericite clusters are pseudomorphs after staurolite. Small subhedral garnets (gt) overgrow the foliation. Plane-polarized light; 8 mm across.

Figure 7. Photomicrographs of pelitic schist cut perpendicular to S_2 and parallel to L_2 showing alteration of porphyroblasts.

2.4 METHODS

Data and samples were gathered in the field from February to November 1992. Mapping was conducted at the scale of 1:3,000 using the USGS 7.5' Ladron Peak quadrangle for a two square mile area in the south-central part of the range (Fig. 3, Plate 1).

The orientations of foliations, lineations, fold hinges, quartz veins, and fractures were measured. Multiple foliations were recognized based on general orientations and overprinting relationships. Oriented samples were collected for microstructural analysis. Sense-of-shear indicators, including S-C fabrics (Berthé et al., 1979a; Lister and Snoke, 1984) and shear bands (Gapais and White, 1982; Gapais, 1989), were examined in thin sections cut parallel to extension lineations and perpendicular to foliations. Attitudes of lineations and poles to foliations were plotted on lower hemisphere equal area net projections. Data were plotted with Fabric, a computer program developed by Starkey (1970, 1977). Starkey (1970) derived the relationship between the percent area of empty space and the percent area occupied by a sample of a given size on the surface of a sphere. Contours represent multiples of random distribution and are weighted according to the percent area in the sphere occupied by the data. Contoured plots of different sample sizes can therefore be compared.

As mentioned earlier, the Ladron Mountains contain tilted (30° W-dipping) Phanerozoic strata which are in unconformable contact with the Proterozoic rocks in the southwestern part of the range (Fig. 3). The rocks of the study area, however, are in fault contact with Phanerozoic strata. The Proterozoic rocks therefore could not be rotated back to Phanerozoic orientations. Structures are discussed in terms of present-day orientations.

Eleven samples collected for U-Pb zircon geochronology were crushed, sieved (<100 mesh), and concentrated at the New Mexico Bureau of Mines and Mineral Resources (NMBMMR) (see Appendix). Zircon was found in only two of these samples. The samples were analyzed at the Massachusetts Institute of Technology in the geochronology laboratory of S.A. Bowring. Preliminary ages of the two samples have been obtained.

3. ANALYTICAL OBSERVATIONS AND RESULTS

3.1 STRUCTURAL ANALYSIS

3.1.1 **Introduction**

Ductile shear zones are recorded by deformational structures. These structures include both linear and planar fabrics associated with varying degrees of ductile flow accommodated along shear planes. The shear zone can develop from a variety of combinations of homogeneous and heterogeneous simple shear and pure shear (Ramsay, 1980).

The two types of linear fabrics observed in this study include crenulation lineations (discussed later) and extension lineations. Extension lineations record the orientation of the maximum stretching direction during progressive ductile deformation and are taken to be subparallel to the transport direction in a shear zone. Because displacement due to simple shear is a major component of most shear zones, determination of the direction of movement along a shear zone is important. When examining shear-sense criteria in shear zones, it is only valid to look at surfaces perpendicular to the foliation and parallel to the extension direction. Extension directions were confirmed by the presence of microstructures which are known to have formed during progressive simple shear. These include mineral lineations, grain elongation, S-C fabrics, C'-surfaces (extensional shear bands), and mica fish. A combination of the following shear-sense indicators was used to verify transport direction.

Cleavage and shear planes are usually found together to form S-C fabrics (Berthé et al., 1979a). C-surfaces are discrete narrow shear zones which lie parallel to the flow plane of the progressive deformation (Fig. 8a). S-surfaces represent a penetratively developed flattening fabric and describe a sigmoid shape between any two adjacent C-surfaces (Fig. 8a). The sigmoid S-surfaces rotate towards the shear plane with increasing strain, and the geometry between the two surfaces reflects the sense of shear.

C'-surfaces (Berthé et al., 1979a) are commonly observed to form after an S-C fabric is developed and indicate some component of pure shear during the progressive deformation (Fig. 8b). C'-surfaces are oriented at

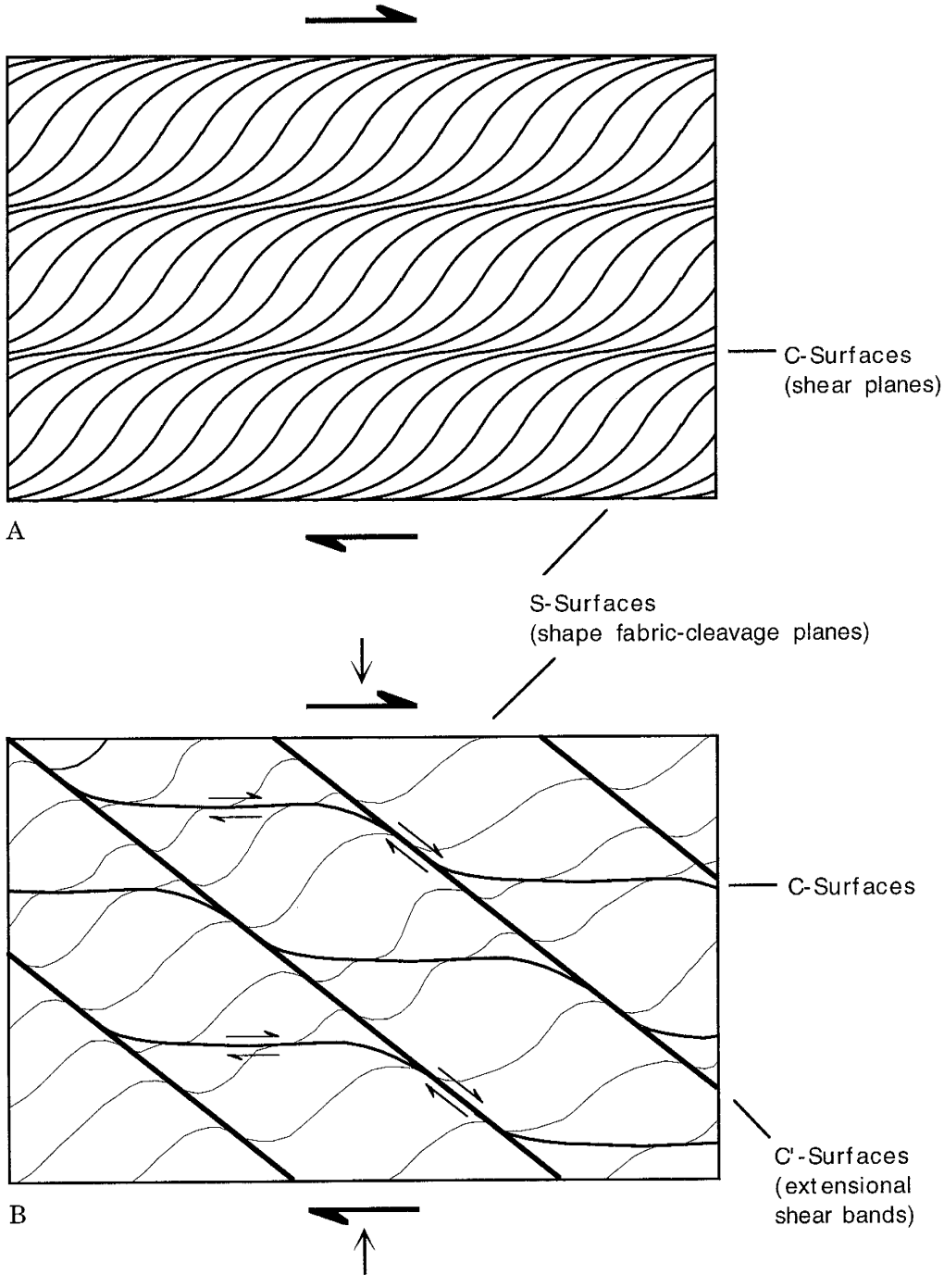

Figure 8. (A) S-C fabric produced by progressive simple shear (modified from Lister and Snoke, 1984. (B) C'-surfaces within an S-C fabric produced by a component of pure shear during the progressive deformation.

15-25° to the bulk flow plane, and the sense of slip is synthetic to the bulk shear sense. Normal movement along the C'-surfaces causes deflection of both S- and C-surfaces to give a reliable sense of shear (Fig. 8b, Fig. 9a). It may not always be possible to distinguish between C- and C'-surfaces if only one of the two is present in a sample. In mica-bearing rocks, the two surfaces can be distinguished from one another; it is common for mica grains to exhibit grain-size reduction along C-surfaces, whereas they tend to be extended and bent into C'-surfaces.

The final shear sense indicator observed in this study is mica fish (Lister and Snoke, 1984). Mica fish are oriented at a small angle to the shear planes, and the 001 cleavage planes of the micas are subparallel to the long dimensions of the fish (Fig. 9b). This angular relationship used with other kinematic indicators provides a valid sense of shear.

Ductile deformational events are associated with certain pressure and temperature conditions. These conditions can be determined on the basis of mineral reactions and phase stabilities if metamorphic mineral assemblages are produced during the deformation. In their absence, such as in quartzofeldspathic rocks, detailed studies of microstructures can provide insight into the temperature conditions of deformation (c.f. Boullier and Bouchez, 1978; Debat et al., 1978; Simpson, 1985). In general, the deformational behavior of feldspars changes from brittle to ductile across the greenschist to amphibolite facies transition. Feldspars in the greenschist facies deform by fracturing and show undulatory extinction and deformation twins. In the amphibolite facies, feldspars deform by microscopically ductile processes resulting in dynamic recrystallization and elongation. Also taking place at these conditions is the formation of strain-related myrmekite on the edges of potassium feldspar porphyroclasts facing the maximum shortening direction (Simpson, 1985). Quartz remains ductile throughout a wide range of temperatures, but microstructures change from monocrystalline quartz ribbons at greenschist facies conditions to quartz ribbons with a granoblastic polygonal microstructure at amphibolite facies conditions. Quartzofeldspathic rocks exhibiting a granoblastic polygonal microstructure generally indicate stable conditions during deformation under amphibolite facies (or higher grade) conditions.

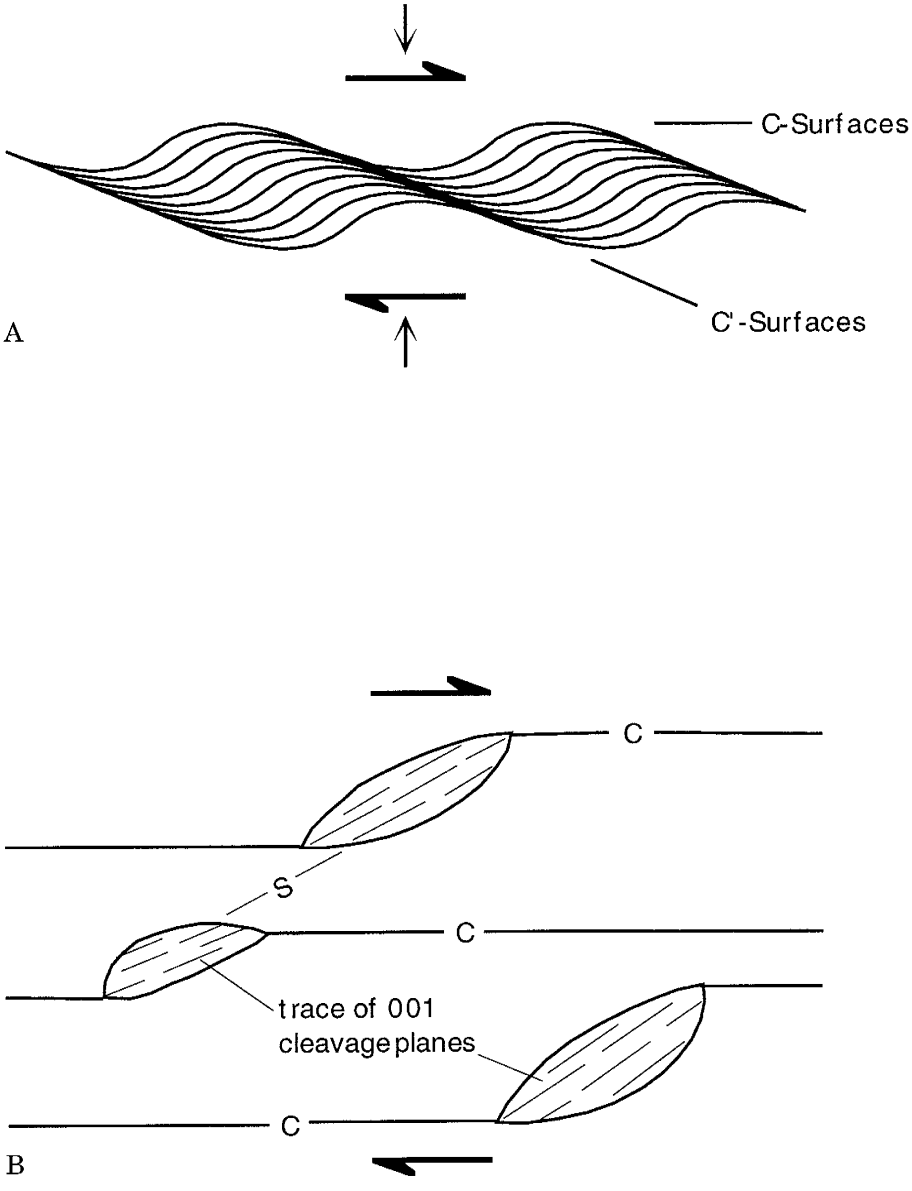

Figure 9. Sense-of-shear indicators found in the deformed rocks of the Ladron Mountains. (A) Diagram of extensional shear bands (from Hanmer and Passchier, 1991). (B) Mica fish (from Lister and Snoke, 1984). The 001 cleavage planes of the mica fish are always oriented subparallel to the long dimension of the fish.

3.1.2 **Deformational Events**

The Proterozoic rocks of the Ladron Mountains contain evidence for two major deformational events. The oldest of these, D_1, is best recorded by structures recognized in the field in the felsic metavolcanic unit (Fig. 4, Plates 1 and 2). From west to east, younger, D_2 structures become increasingly well developed throughout the field area. D_2 structures are best developed in the eastern metamorphic sequence. The incomplete overprinting of D_1 structures by D_2 structures provides an opportunity to characterize two distinct Proterozoic deformational events, both of which postdate extrusion of the felsic metavolcanic unit and intrusion of the Bandit granophyre. There is also local evidence for both ductile and brittle post-D_2 deformation. The notation used for deformational events and associated structures in the Ladron Mountains is given in Table 1.

Table 1. Structural notation.

	STRUCTURES			
EVENT	Foliation	Extension Lineation	Crenulation Lineation	Fold Generation
D_1	S_1	L_1	none observed	none observed
D_2	S_2	L_2	in S_1	F_2
post-D_2	none observed	none observed	in S_2	post-D_2

Foliations were distinguished as S_1 and S_2 in the field primarily on the basis of orientation and crosscutting relationships, rather than on structural characteristics. It is common for two or three types of planar fabrics to be present in a single unit, but only the orientation of the macroscopically observable foliation was measured and labeled as either S_1 or S_2. Also, orientations of S_1 in the clastic metasedimentary and eastern metamorphic sequences have not been determined due to overprinting by S_2. S_1, everywhere, is the oldest observable fabric; S_1 in the supracrustal sequence is interpreted to be equivalent to S_1 in the felsic metavolcanic unit. Four basic types of planar fabrics have been distinguished both

macroscopically and microscopically. These are crenulation cleavages, cleavage planes (S-surfaces), shear planes (C-surfaces), and extensional shear bands (C'-surfaces). While the latter foliations were described in the previous section, crenulation cleavages have not been discussed. A crenulation cleavage develops through the deformation of a pre-existing fabric through pure shear, simple shear, or a combination of the two. Figure 10 shows the hypothetical development through progressive simple shear of a crenulation cleavage from open crenulations in an older foliation (Stage 1) into a penetrative foliation (Stage 6) at the microscopic scale. Stage 3 shows alternating mica-rich and quartz-rich layers inferred to have been produced by rotation of older micas during dextral shear and mass transfer of quartz from fold limbs to hinges. This stage also includes preferential growth of micas, predominantly in mica-rich layers, during dextral shear. In Stage 4, continued shear causes rotation of the new mica grains parallel to the crenulation cleavage, axial planar to the crenulations. Stage 5 shows destruction of the relict crenulations, in which rare mica grains in the quartz-rich layers have grown parallel to the crenulation cleavage. In Stage 6, repartitioning of quartz and mica (via dissolution and mass transfer ?) has produced a homogeneous foliation.

The presence of sense-of-shear indicators in the Proterozoic rocks of the Ladron Mountains indicates that a component of simple shear was involved in the formation of the fabrics. As noted earlier, shear bands form when there is also a component of pure shear. Therefore, this suggests that components of both simple and pure shear operated during fabric development in the Ladron Mountains. The relative importance of each cannot be accurately assessed from the data available, although there is little evidence for extensive shortening during either D_1 or D_2. In the following sections, attention is focused on evidence of simple shear with the understanding that a component of pure shear was involved in fabric development.

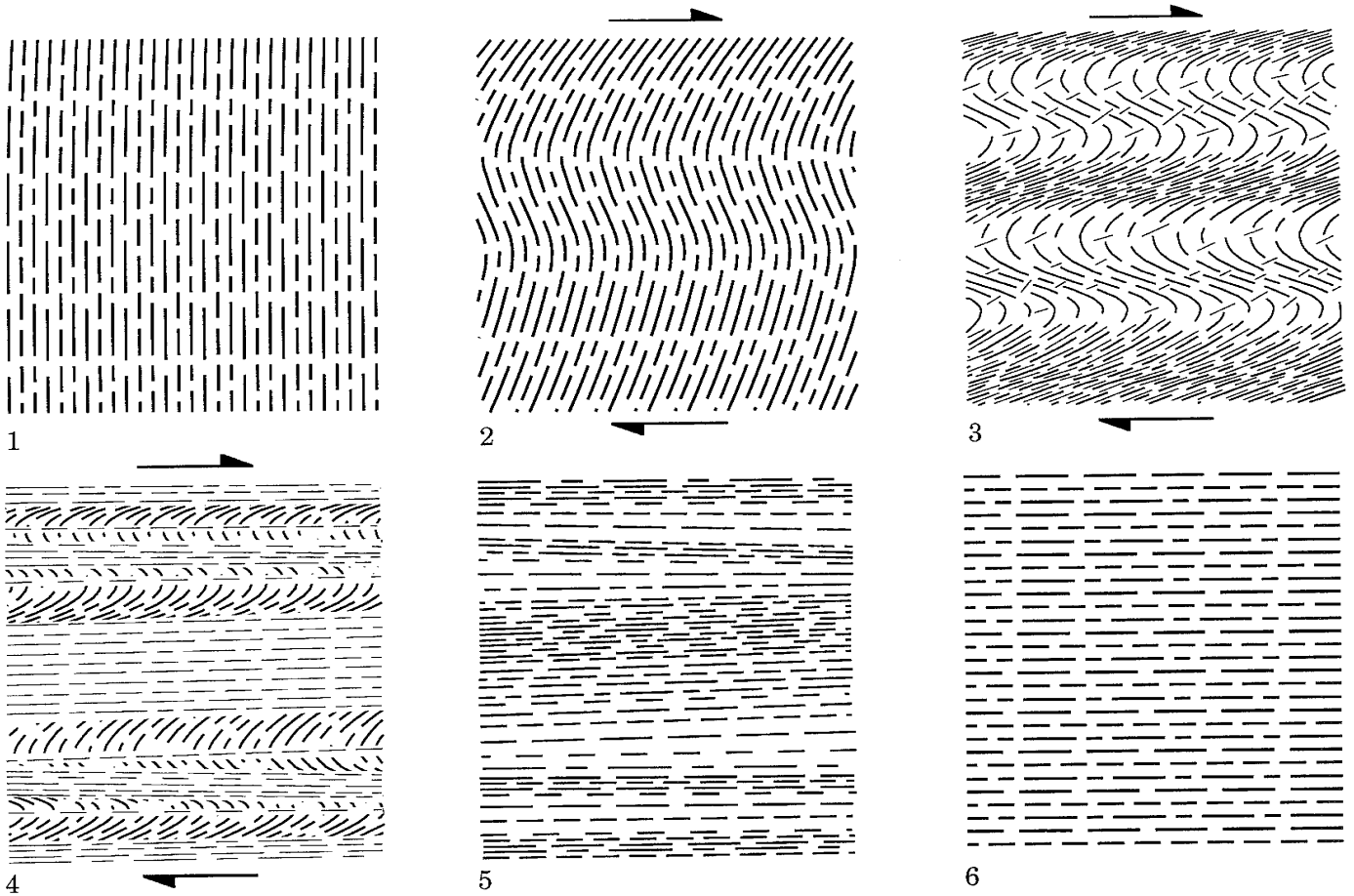

Figure 10. A hypothetical example of six stages of development of a new schistosity via a crenulation cleavage at the microscopic scale. Stage 1 shows the original foliation. Stage 2 shows crenulation of the foliation during progressive simple shear. Stage 3 shows crenulation accompanied by preferential mica growth and consequent metamorphic differentiation. Stage 4 shows rotation of new micas parallel to the new schistosity and axial planar to crenulations. Stage 5 shows destruction of relic crenulations in quartz domains. Stage 6 shows homogenized schistosity (modified from Bell and Rubenach, 1983).

3.1.3 D_1 Event

3.1.3.1 Field Relationships

The main structure that records D_1 deformation is a foliation, S_1 (Fig. 11). S_1 is a subvertical, WNW-striking foliation, which is best developed throughout the felsic metavolcanic unit. It is moderately well expressed in the Bandit granophyre and poorly expressed in the meta-arkose. These three units contact at a "triple point" in the northwestern part of the study area (Fig. 4, Plate 1). The Bandit granophyre borders the felsic metavolcanic unit to the north, while the meta-arkose borders it to the south. These two contacts dip steeply (Plates 1 and 2). The contact between the Bandit granophyre and the meta-arkose is not exposed. The character of these contacts is discussed below. Primary layering has not been identified in the felsic metavolcanic unit, and S_1 is not parallel to bedding in the meta-arkose. In one outcrop where S_1 is preserved within the ultramylonite unit, it is defined by alternating quartz-rich and white mica-rich compositional layers.

3.1.3.2 Microstructures and Sense-of-Shear Indicators

S_1 is defined by the preferred dimensional alignment of white mica and biotite. Locally, this alignment occurs along shear planes (C-surfaces). In general, the spacing between foliation surfaces ranges from up to 1 mm in the felsic metavolcanic unit to up to 1 cm in the Bandit granophyre and meta-arkose. Shape fabrics (S-surfaces) are rare; quartz and feldspar grains generally have a granoblastic polygonal microstructure and show very little elongation. A photomicrograph of the Bandit granophyre (Fig. 12) exhibits these features as well as a rare S-C fabric defined by micas and associated shear bands within fine grained quartz domains.

Mineral assemblages (quartz >> K-feldspar + plagioclase ± mica) within the felsic metavolcanic unit, Bandit granophyre, and meta-arkose are similar and do not constrain the P-T conditions of deformation. However a detailed study of the microstructures can provide insight into the metamorphic conditions of deformation. Microstructures in feldspars from all three rock types indicate that subgrain formation, recrystallization, kinking, deformation twinning, strain-related myrmekite

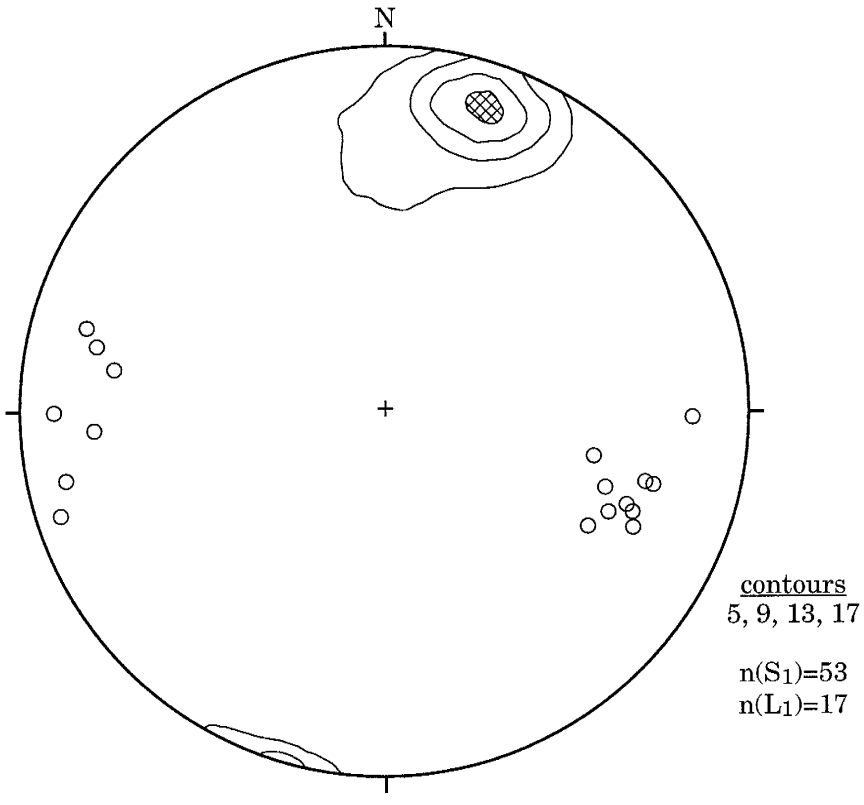

Figure 11. Lower hemisphere equal area projection of L_1 (○) and poles to S_1 (contoured) in the felsic metavolcanic unit, meta-arkose, and Bandit granophyre. The area of the diagram below the lowest specified contour is blank; the area above the highest contour is cross-hatched.

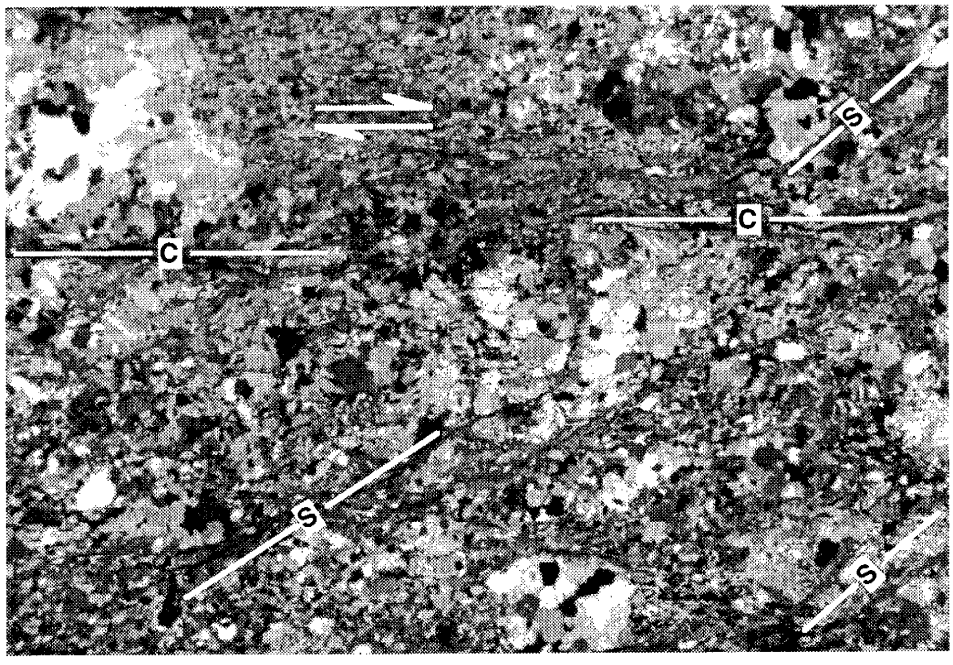

A. S-surfaces are defined by micas, which show anastomosing behavior around large recrystallized quartz and feldspar porphyroclasts. C-surfaces are the macroscopically observable foliation. 1/4 wave plate.

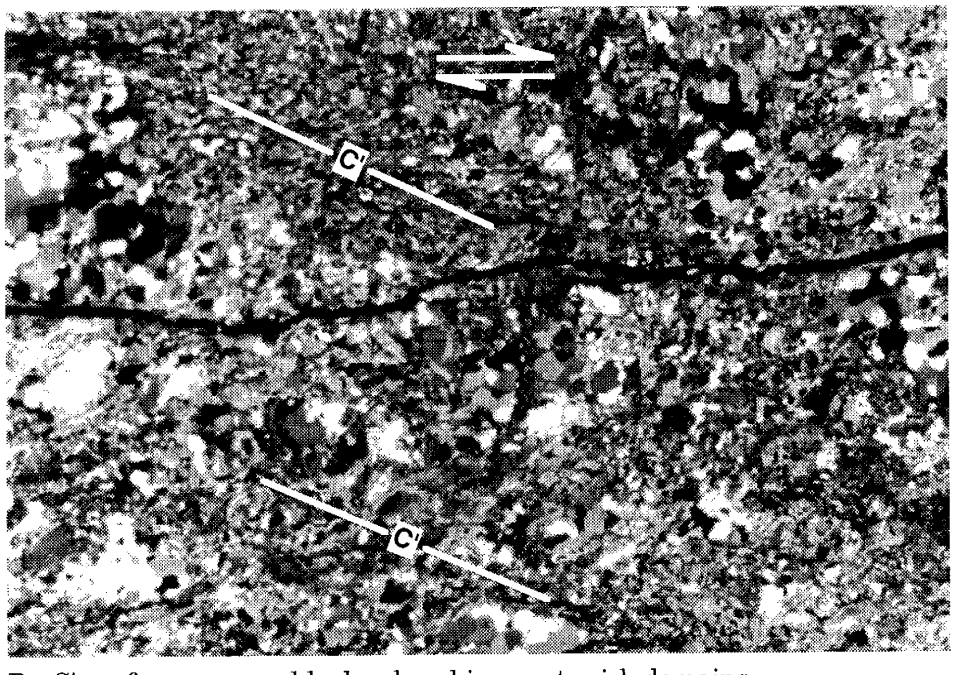

B. C'-surfaces are weakly developed in quartz-rich domains.

Figure 12. Photomicrograph of Bandit granophyre cut perpendicular to S_1 and parallel to L_1. (A) S-C fabric (shown in color) and (B) C'-surfaces (shown in black and white) indicate dextral shear. Crossed polars; 8 mm across.

formation, and boudinage all accommodated deformation. Grains may be elongate and exhibit undulatory extinction. Quartz grains are equant and show undulatory extinction and straight to sutured grain boundaries. Symmetric and asymmetric polycrystalline quartz augen are common. Intracrystalline cataclasis (Goodwin and Wenk, 1990) and kinking are common in coarse biotite grains. These observations are consistent with deformation under amphibolite facies conditions. Extensive sericitization of feldspars suggests the presence of fluids. Fluids must have been present prior to or during deformation, as sericitized feldspar grains are more strongly deformed than unaltered grains. The occurrence of more total sericite at the expense of feldspar also explains the abundance of quartz porphyroclasts relative to feldspar porphyroclasts.

Lineations (L_1) in the felsic metavolcanic unit and the Bandit granophyre are defined by elongate quartz grains, and less frequently elongate feldspar grains, and a preferred dimensional alignment of white mica and biotite. L_1 is therefore interpreted as a stretching lineation. In both units, L_1 plunges shallowly (Fig. 11). Kinematic indicators (n=7) including S-C fabrics and shear bands found in the Bandit granophyre (Fig. 12) and the felsic metavolcanic unit indicate dextral strike-slip movement along the NW-oriented shear planes. No extension lineations were observed in S_1 in the meta-arkose.

3.1.3.3 Contact Relationships and Strain Partitioning

Contact relationships between the various rock units of the Ladron Mountains have been discussed under Previous Studies. Further discussion will be devoted to the contacts between the felsic metavolcanic unit and both the meta-arkose and Bandit granophyre where relative age relationships are uncertain.

Felsic metavolcanic unit / Bandit granophyre contact

In outcrop adjacent to the Bandit granophyre, foliation surfaces in the felsic metavolcanic unit anastomose around irregularly shaped pods of the Bandit granophyre (Fig. 13a). Microstructures within the Bandit granophyre at this contact include sericitized feldspars and recrystallized feldspar and quartz porphyroclasts in a very fine-grained matrix of the two

A. Large, irregularly shaped pod of bg incorporated into fmv adjacent to the contact. 1 meter across.

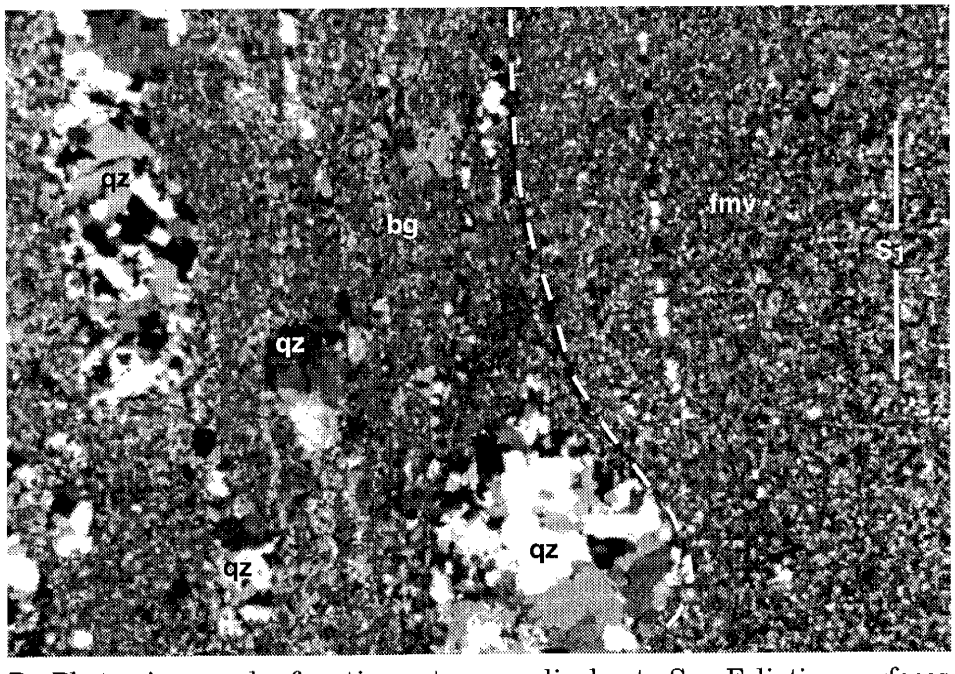

B. Photomicrograph of section cut perpendicular to S_1. Foliation surfaces in the fmv and bg are parallel to the contact (dashed). Bg matrix is fine grained and contains recrystallized elongate and rounded clasts parallel to both S_1 and the contact. Crossed polars; 8 mm across.

Figure 13. Structural relationships between the Bandit granophyre (bg) and the felsic metavolcanic unit (fmv).

minerals. The change from a medium grained rock away from the contact to this fine-grained microstructure reflects grain-size reduction. As previously noted, sericitized feldspars deform more readily than unaltered grains. This suggests that enhanced deformation due to sericitization (and/or complete alteration to sericite) has diminished the number of feldspar porphyroclasts relative to quartz porphyroclasts. In addition, the remnant recrystallized quartz porphyroclasts in the Bandit granophyre are elongate parallel to the contact, and also to S_1, as shown in the photomicrograph in Figure 13b. These observations collectively suggest that this contact accommodated shearing during D_1 and therefore is tectonic in character.

Felsic metavolcanic unit / meta-arkose contact

In outcrop adjacent to the meta-arkose, foliation surfaces in the felsic metavolcanic unit anastomose around irregularly shaped pods of meta-arkose (Fig. 14a). The remnant pods are subangular to subrounded, and are generally not elongate parallel to S_1. The meta-arkose adjacent to this contact is composed dominantly of a very fine-grained matrix of quartz and feldspar, which surrounds recrystallized clasts of the two minerals (Fig. 14b). The matrix here is much finer-grained than away from the contact. In the photomicrograph in Figure 15, S_2 is locally subparallel to this contact, and S_1 is at a moderate angle (~45°) to, and appears truncated by, the contact. This is consistent with the change in orientation of the contact from west to east (Fig. 4). To the west, the trace of the contact is subparallel to the strike of S_1 but curves up into parallelism with the strike of S_2 to the east. Furthermore, the strike of S_1 has also rotated toward the strike of S_2 towards the east. This contact therefore is interpreted to be tectonic in character.

Bandit granophyre / meta-arkose contact

Although this contact is not exposed, the following observations suggest it is also tectonic in character. First, there is evidence of grain-size reduction in the meta-arkose adjacent to the contact. Microstructures are similar to those described above (e.g., relict porphyroclasts within a fine-grained matrix), but grain-size reduction has not been as intense as was

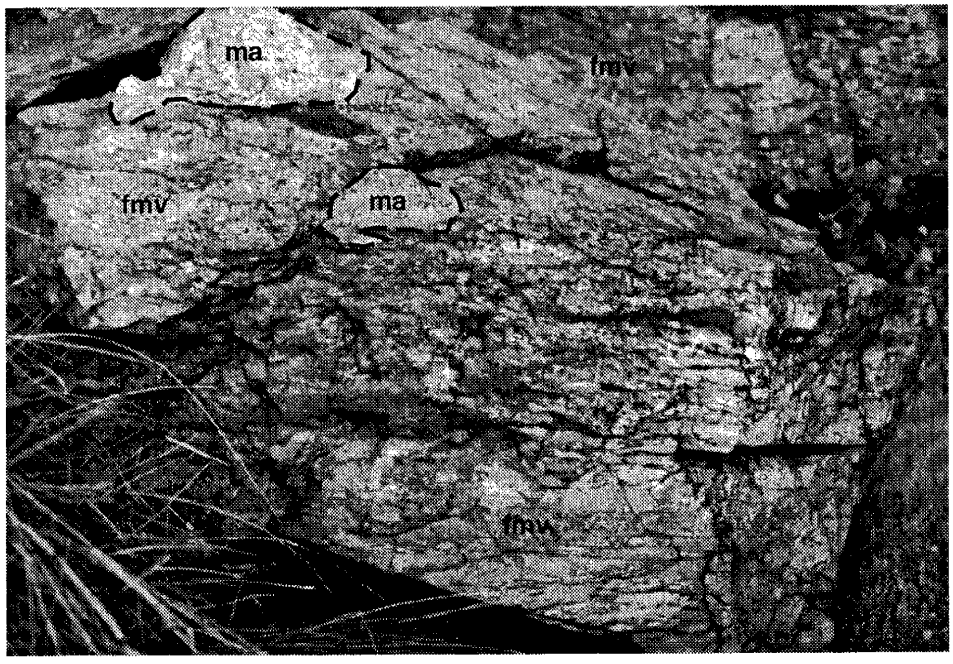

A. Irregularly shaped pods of ma incorporated into fmv. 1 m across.

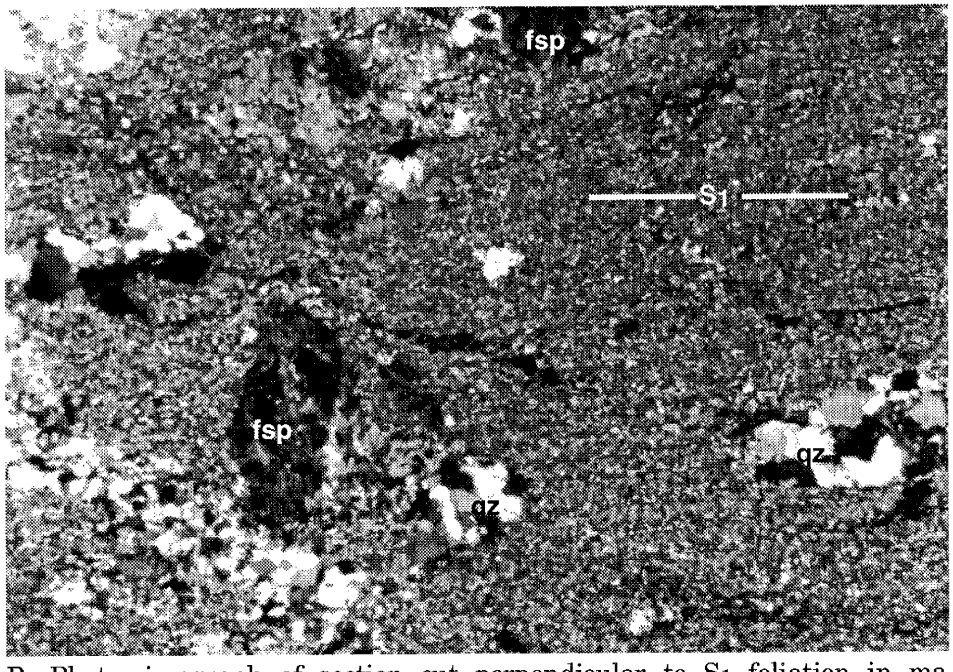

B. Photomicrograph of section cut perpendicular to S_1 foliation in ma adjacent to fmv. Foliation surfaces are not well delineated and the ma matrix is extremely fine grained. Recrystallized quartz and feldspar porphyroclasts are subrounded to subangular and show no preferred orientation with respect to S_1. Crossed polars; 8 mm across.

Figure 14. Structural relationships between the meta-arkose (ma) and the felsic metavolcanic unit (fmv).

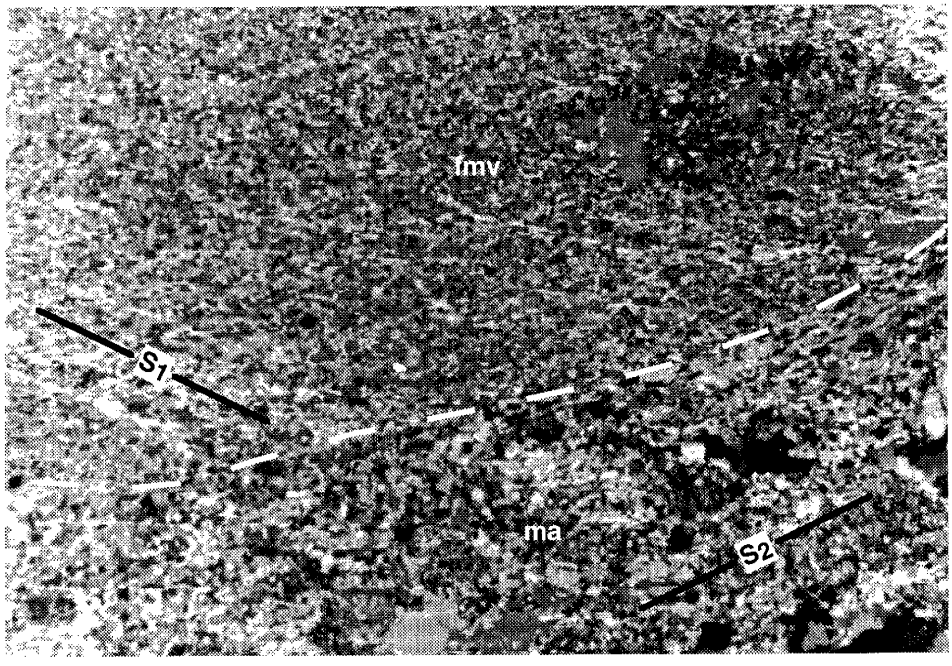

Figure 15. Photomicrograph of contact between the meta-arkose (ma) and the felsic metavolcanic unit (fmv) cut perpendicular to S_1. S_2 is subparallel to the contact (dashed). Crossed polars, 8 mm across.

observed at the other two contacts. The Bandit granophyre, however, does not exhibit evidence of grain-size reduction adjacent to the contact. Moreover, it is observed to be rather weakly deformed in a few outcrops, which illustrates the heterogeneous nature of structures developed in this rock. Second, the trace of the contact is a continuous extension of the felsic metavolcanic unit/meta-arkose contact to the south, and is generally parallel to the strike of S_2. This suggests that: (1) shearing associated with the felsic metavolcanic unit/meta-arkose contact also occurred here and (2) this movement occurred during D_2.

Strain Partitioning

The triple point geometry between these three units is defined by the intersection of the felsic metavolcanic unit/Bandit granophyre contact with the western contact of the meta-arkose. The general parallelism of S_1 with the former and S_2 with the latter, in addition to the structural relationships outlined above, indicates movement along these contacts during D_1 and D_2, respectively. As previously noted, the degree of development of S_1 varies from one unit to the other. Adjacent to the felsic metavolcanic unit, microstructures within the meta-arkose and Bandit granophyre are similar, but grain-size reduction was greater in the Bandit granophyre with only a few porphyroclasts surviving. S_1 is more strongly developed here than adjacent to the contact between the meta-arkose and felsic metavolcanic unit. In addition, as shown on the geologic map (Fig. 4, Plate 1), the felsic metavolcanic unit experienced virtually no strain during D_2. These observations suggest that strain was concentrated along the western contact of the meta-arkose and in the supracrustal rocks to the east during D_2.

3.1.4 **D_2 Event**

3.1.4.1 Field Relationships

The dominant foliation in the study area, S_2 (S_1 of Taylor, 1986), is well developed throughout the entire eastern supracrustal package (excluding the meta-arkose) (Fig. 4, Plate 1). S_2 is parallel to bedding in the clastic metasedimentary sequence, but at an angle (10-15°) to compositional layering in the pelitic schist. This may indicate

transposition of layering as discussed below. S_2 is moderately developed in the meta-arkose and only locally developed in the Capirote pluton and the Bandit granophyre. In the felsic metavolcanic unit, S_2 is locally weakly developed to absent. Throughout the study area, S_2 strikes NE and dips moderately to the SE (Fig. 16). It is best developed in the eastern metamorphic sequence where white mica, biotite, and blue-green amphibole are the main foliation-forming phases, and where overprinting of S_1 by S_2 is relatively advanced. Where S_1 is not fully overprinted, S_2 is locally observed to be a crenulation cleavage. S_2 orientations in the Bandit granophyre and meta-arkose deviate slightly from the norm and are more northerly-striking and dip more steeply to the SE as shown with the equal area net in Figure 16b. This variation in the orientation of S_2 may reflect the incipient stage of development of S_2 in the Bandit granophyre and meta-arkose. The larger grain size and greater competence of these lithologies may have hindered the progressive development of S_2. It is reasonable to expect the less competent lithologies to accommodate more of the strain.

In the Capirote pluton, S_2 is a mylonitic foliation found in discrete shear zones defined by elongate polycrystalline quartz lenses and by rare elongate feldspar grains. There are two types of shear zone. In the first, grain size changes abruptly from medium grained in the host rock to very fine grained in these usually narrow (1-5 cm), anastomosing shear zones. Another type of mylonitic shear zone found in the pluton is localized along pre-existing quartz veins. The quartz monzonite mylonites (qm-mylonites) have two sets of orientations, one of which is identical to the dominant S_2 orientation (Fig. 16a); the other set strikes NW and dips to the NE (Fig. 17a). The quartz vein mylonites (qv-mylonites) also strike NW, but dip to the SW (Fig. 17b). The two NW-striking shear zones are oriented such that they may represent a conjugate shear pair (Fig. 17; Plates 1 and 2). Although cross-cutting relationships between the NE- and both NW-striking shear zones were not observed, microstructural observations (discussed below) suggest that they both formed during D_2.

Intrusive and crosscutting relationships were also observed in reference to D_2 fabrics. Undeformed pegmatite/aplite veins associated with the Ladron pluton crosscut the mylonitic shear zones in the Capirote pluton and foliations in the metamorphic suite. The foliation in the

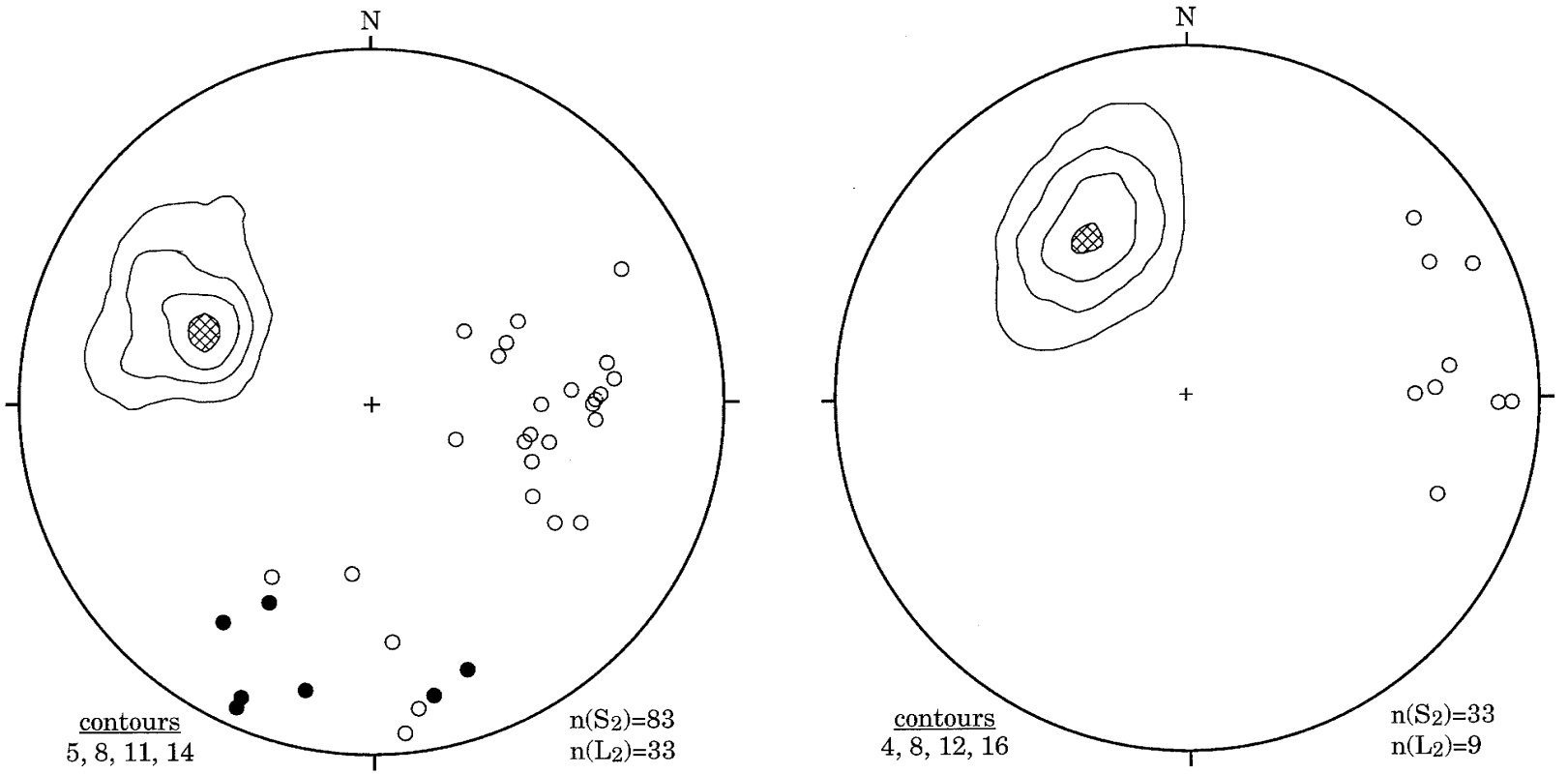

A. Supracrustal rocks (○) (except meta-arkose) and NE-striking qm-mylonites (●).

B. The meta-arkose and Bandit granophyre.

Figure 16. Lower hemisphere equal area projection of L_2 (circles) and poles to S_2 (contoured) of the supracrustal sequence, the Capirote pluton, and the Bandit granophyre. The area of the diagram below the lowest specified contour is blank; the area above the highest contour is cross-hatched.

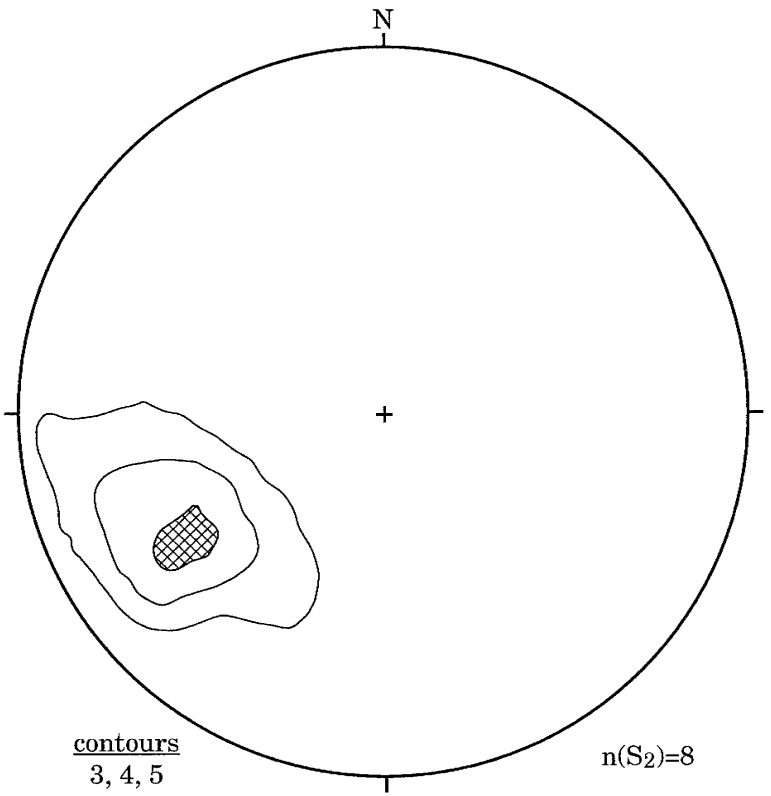

A. NW-striking qm-mylonites.

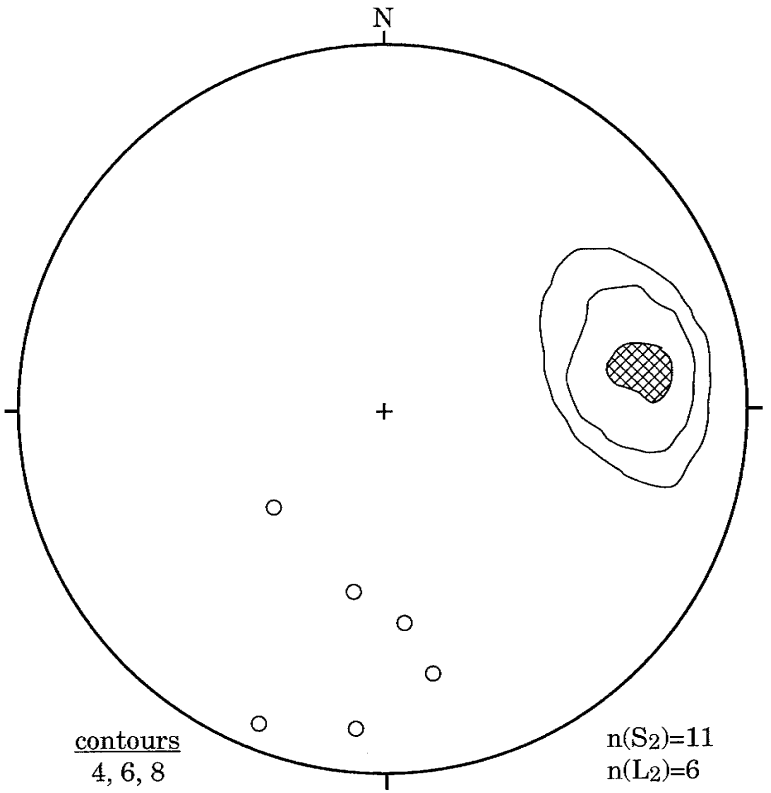

B. Qv-mylonites.

Figure 17. Lower hemisphere equal area projection of L_2 (circles) and poles to S_2 (contoured) in the Capirote pluton shear zones. The area of the diagram below the lowest specified contour is blank; the area above the highest contour is cross-hatched.

ultramylonite is at a high angle to the contact with the white phase of the Ladron pluton and is abruptly truncated at this margin (Fig. 18). Contact metamorphic aureoles were not recognized in the supracrustal rocks adjacent to either the Capirote or the Ladron pluton.

Stretching lineations (L_2) were observed in all units except for the felsic metavolcanic unit and the NW-striking qm-mylonites. L_2 is defined by the preferred dimensional alignment of micas and amphiboles in the pelitic schist and amphibolites, and by elongate feldspar porphyroclasts and polycrystalline quartz ribbons in the clastic metasedimentary sequence, the ultramylonite, and the plutonic rocks. Two plots of L_2 are shown in Figure 16; the Bandit granophyre and meta-arkose were plotted separately due to a slightly different orientation of S_2. In Figure 16a, two orientations of L_2 within the supracrustal rocks and the qm-mylonites are evident: moderately E-plunging and more shallowly S-plunging. It is important to note that the S-plunging lineations are not localized within a geographically distinct area and are present in both the supracrustal sequence and the Capirote pluton. In the qv-mylonites, L_2 plunges moderately to the south (Fig. 17b), similar to orientations in the qm-mylonites. Overall, in the supracrustal rocks the E-trending lineations are dominant, whereas in the Capirote mylonites L_2 is S-trending (Figs. 16a and 17b).

D_2 folds were observed locally where incomplete overprinting of S_1 by S_2 occurred. In these few instances, S_1 forms tight to isoclinal folds (F_2) in the quartzite (Fig. 19a) and ultramylonite units, with S_2 axial planar to the hinges. These F_2 fold hinges plunge moderately within the SE quadrant of the equal area net (Fig. 19b).

3.1.4.2 Microstructures

S_2 is defined by the preferred dimensional alignment of white mica, biotite, and amphibole. This alignment dominantly occurs along C-surfaces where these minerals have rotated into the shear planes and exhibit grain-size reduction. The spacing between C-surfaces changes from less than 1 mm in the pelitic schist to nearly 1 cm in the clastic metasedimentary units. This can be attributed to variations in competence between lithologies. Potassium feldspar porphyroclasts in the

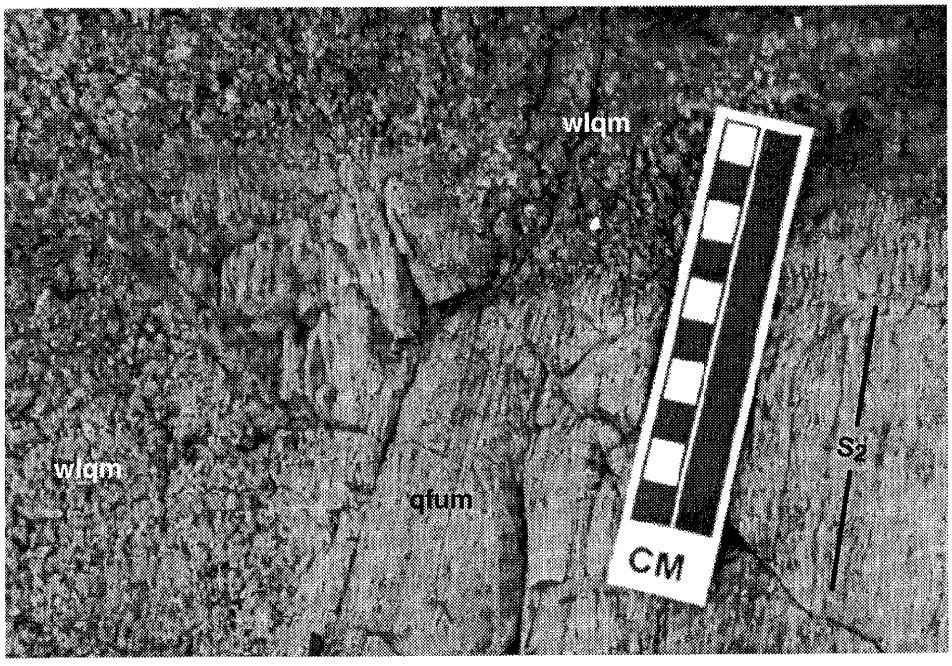

Figure 18. Intrusive and structural relationships between the white phase Ladron pluton (wlqm) and the quartzofeldspathic ultramylonite (qfum). Truncation of foliation (S_2) in qfum along margin of wlqm. View looking down at an angle to foliation surfaces, which dip off to the right (southeast); cm bar for scale.

A. F_2 folds in quartzite showing crenulation of S_1 surfaces and development of S_2 crenulation cleavage (horizontal) axial planar to fold hinges. View looking to the east; 1 m across.

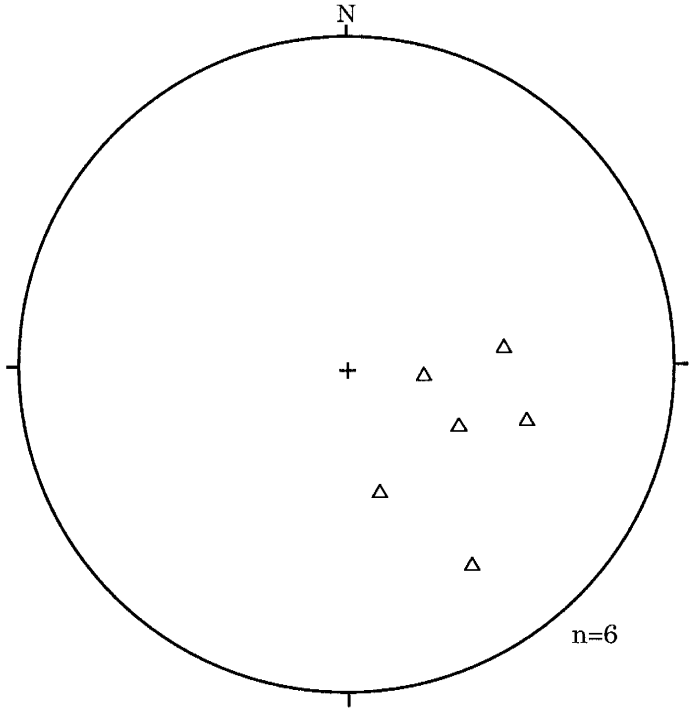

B. Lower hemisphere equal area projection of F_2 hinges (△).

Figure 19. Relationships and orientations of F_2 hinges in the supracrustal sequence.

meta-arkose and Bandit granophyre locally contain strain-related myrmekite, indicative of deformation at amphibolite facies conditions (Simpson, 1985). In the pelitic schist, S_2 is locally at an angle (~30°) to compositional layering and intrafolial folds in the ultramylonite were locally observed (Fig. 20). However, the importance of transposition of bedding cannot be accurately assessed because of the insufficient number of features observed including repetition of layers. As noted earlier, mineral assemblages in the pelitic schist and garnet-biotite geothermometry indicate amphibolite facies metamorphism during D_2. Structural relationships within the supracrustal rocks are similar, as described below.

S_1 is consistently overprinted by S_2. Relict S_1 foliation-forming minerals (white mica and amphibole) are locally oriented at a high angle to S_2. These relict mineral grains are relatively small, deformed, and are truncated by S_2 surfaces. Several examples illustrate this overprinting relationship, as well as the relative timing of metamorphism and development of S_2. Locally, in the pelitic schist, strongly deformed white mica grains between closely spaced C-surfaces (< 1 mm) are consistently oriented perpendicular to the C-surfaces. These white mica grains must have grown prior to D_2 and defined an earlier foliation (S_1). Microstructures in the amphibolites are similar, except that the relict S_1 mineral and the S_2 foliation-forming mineral is amphibole. The preferred dimensional alignment of amphibole needles, the majority of which define a mineral lineation, indicates growth of amphibole during D_2.

A photomicrograph of the ultramylonite (Fig. 20) cut perpendicular to the foliation and fold hinge clearly illustrates overprinting of S_1 by S_2. F_2 fold hinges in the ultramylonite are domains where S_1 and compositional layering are folded. Within these hinge areas, mica-rich layers exhibit grains that are bent and oriented at a high angle to S_2. Also in the hinge area, the quartz-rich layers contain grains that have a greater amount of undulatory extinction and sutured grain boundaries. Elsewhere, microstructures record deformation of S_1 by shear along S_2 planes during initial stages of S_2 development (see Fig. 10). Growth and alignment of white mica is evident along these S_2 surfaces.

Porphyroblast-matrix relationships in the pelitic schist provide evidence of the relative timing of metamorphism and deformation. These include mineral growth pre-D_2 and post-D_2. Many garnet and biotite

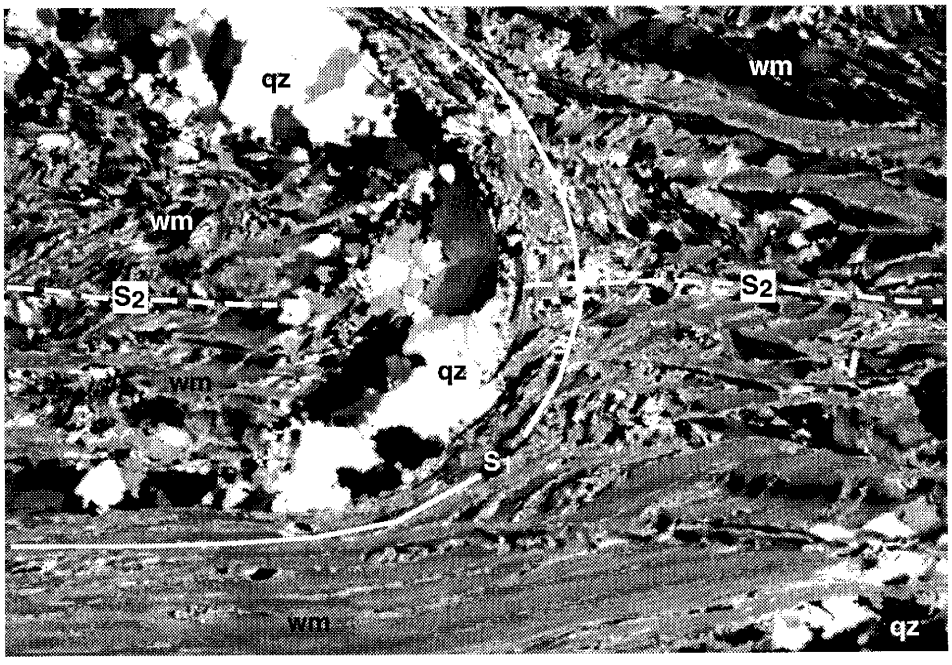

Figure 20. Photomicrograph of ultramylonite cut perpendicular to S_2 and F_2 hinge. S_1 compositional layering is folded and S_2 crenulation cleavage in white mica (wm) domains is axial planar to F_2. Undulatory extinction and recrystallization of quartz (qz) is evident in hinge. View looking to the northwest; crossed polars; 8 mm across.

porphyroblasts contain mineral inclusion trails (generally straight) at a high angle to the main external foliation (S_2), suggesting static overgrowth of a pre-existing foliation (S_1). Other smaller garnet porphyroblast have no inclusion trails and are highly fractured and extended parallel to L_2 along shear planes. This is evidence both for garnet growth pre-S_2 and for the lineation being a stretching lineation. Still other smaller garnet grains are inclusion-free, euhedral, and overgrow the main foliation as indicated by truncation of S_2 against garnet faces. Staurolite is only locally present; where it is seen, it is virtually completely replaced by sericite (Fig. 7b). The morphology of these sericite clusters, observed in outcrop throughout the pelitic schist, suggests that they have replaced individual prismatic crystals 1 to 3 cm in length which were randomly oriented within S_2. The clusters are interpreted as pseudomorphs after relatively large staurolite porphyroblasts and are inferred to have grown statically following development of S_2; S_2 planes are not deflected at the pseudomorph boundaries. These observations suggest that staurolite growth post-dated D_2, and retrogression to sericite occurred subsequently. Thus, these microstructural relationships suggest that amphibolite facies metamorphism outlasted D_2.

In the qm-mylonites, feldspar and quartz microstructures record recrystallization, subgrain development, and grain elongation. Feldspars also show dramatic grain size reduction. Both minerals locally show a granoblastic polygonal microstructure. Therefore, amphibolite grade deformation is interpreted to have accompanied Capirote mylonite formation.

In the qv-mylonites, relatively large, inequant quartz grains have straight to sutured grain boundaries along which subgrain development and recrystallization are apparent (Fig. 21a). These grains also record two distinct sets of mutually perpendicular deformation bands (Fig. 21a), and as can be seen with a gypsum plate, there is a strong crystallographic preferred orientation of quartz grains. Another sample contains monocrystalline quartz ribbons which define an S-surface (Fig. 21b). Parallel to S-surfaces, small lenses and fingers of the quartz monzonite incorporated into the veins are extremely fine-grained, indicating dramatic grain-size reduction (Fig. 21b). The deformation microstructures suggest a very complex history for these quartz veins. However, the monocrystalline

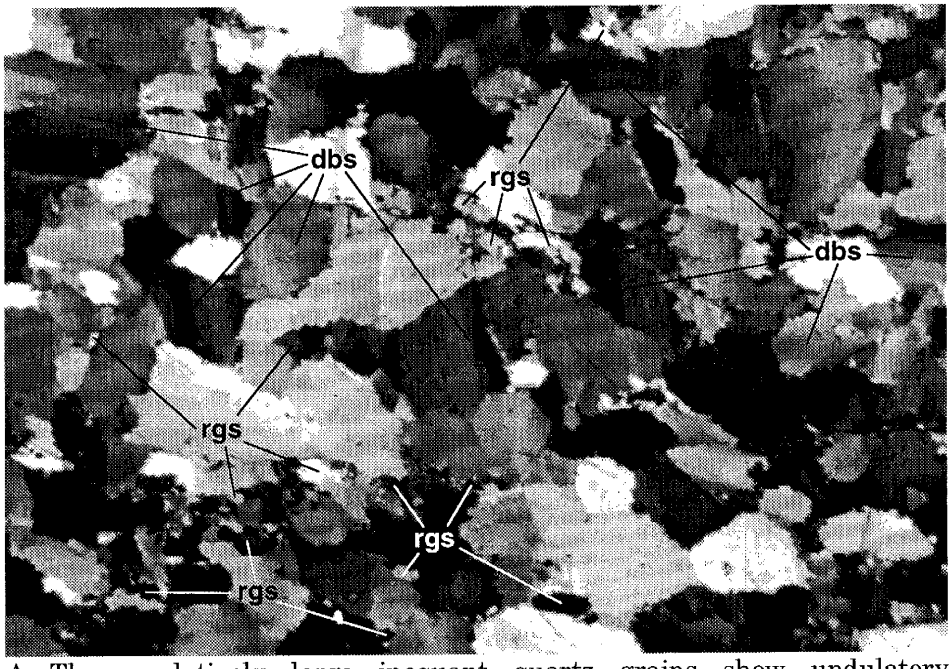

A. These relatively large inequant quartz grains show undulatory extinction, straight to sutured grain boundaries along which are recrystallized smaller grains (rgs), and two sets of mutually perpendicular deformation bands (dbs).

B. Lens of mylonitized quartz monzonite (qm) parallel to S-surface expressed by elongate quartz grains.

Figure 21. Photomicrographs of a qv-mylonite in the Capirote pluton cut perpendicular to S_2 and parallel to L_2. Crossed polars; 8 mm across.

quartz ribbons found in two samples do suggest relatively low temperature conditions, and may record a local overprint. Amphibolite facies conditions are inferred from the microstructures in the qm-mylonites.

3.1.4.3 Sense-of-Shear Indicators

Extension lineations (L_2) are defined by extended feldspar porphyroclasts, elongate quartz grains, polycrystalline quartz ribbons, recrystallized elongate quartz augen, and preferred crystallographic alignment of micas and amphiboles.

Reliable sense-of-shear indicators were found in the clastic metasedimentary sequence, the eastern metamorphic sequence, and the Capirote mylonites. Thin sections were cut parallel to L_2 and perpendicular to S_2. Observed sense-of-shear indicators include S-C fabrics, shear bands, and mica fish (Fig. 22). Where L_2 is E-trending, kinematic indicators in the supracrustal rocks (n=6) show dominantly normal motion with a sinistral component. This motion may have caused the apparent deflection of the strike of S_1 into parallelism with the strike of S_2 at the felsic metavolcanic unit/meta-arkose contact as previously noted. Where L_2 trends south, the sense of shear recorded by fabrics in the supracrustal rocks (n=3) and the qm-mylonites (n=3) is oblique, with dextral and normal components. In the qv-mylonites, shear sense indicators (n=3) show oblique motion with sinistral and normal components. The apparent difference in shear sense in the S-trending lineations, dextral-normal versus sinistral-normal, is the result of the orientation of S_2 in the qv-mylonites (NW-striking, SW-dipping) relative to the supracrustal rocks and qm-mylonites (NE-striking, SE-dipping). In general, the S-trending lineations in both foliation orientations record similar movement directions. In all cases there is a normal component of shear associated with development of S_2 and L_2.

3.1.5 **Post-D_2 Events of Unknown Age**

3.1.5.1 Field Relationships

Locally developed post-D_2 macroscopic structures include: (1) weakly aligned chlorite porphyroblasts which overprint S_2 in the pelitic schist, and (2) open folds in S_2 in the metamorphic sequence (Fig. 23a),

A. Post-D_2 open folds in S_2 in the amphibolite. View looking down on a horizontal surface and perpendicular to foliation; pencil for scale.

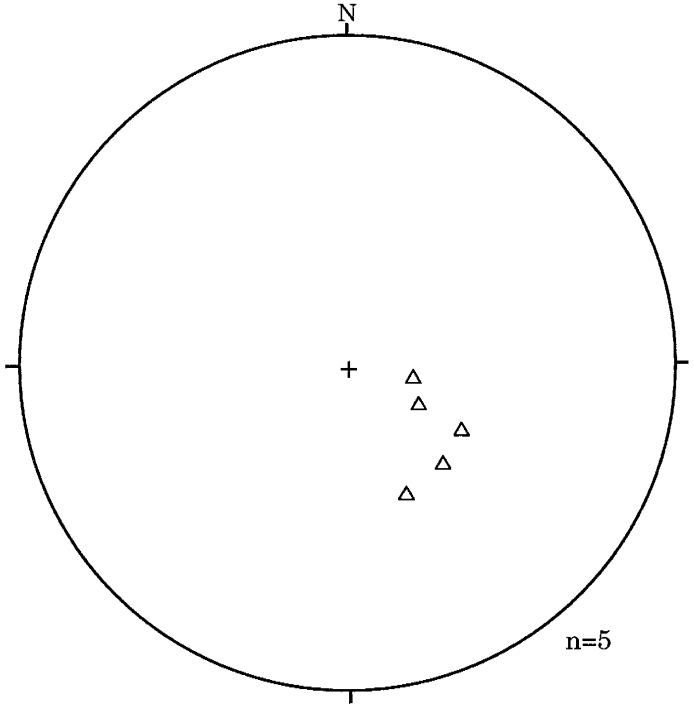

B. Lower hemisphere equal area projection of post-D_2 hinges (△).

Figure 23. Relationships and orientations of post-D_2 hinges in the supracrustal sequence.

metaconglomerate, and quartzite units to produce open folds. Post-D_2 fold hinges plunge steeply to the SE (Fig. 23b).

3.1.5.2 Microstructures

Post-D_2 microstructures are variably developed in the pelitic schist, in qv-mylonites, and in the Ladron pluton. In the pelitic schist, a few features are evident locally in sections cut perpendicular to S_2 and parallel to L_2. In one sample, chlorite porphyroblasts overgrow S_2 and are preferentially aligned with their basal planes at moderate angles (40-70°) to S_2 (Fig. 24a). In another sample, both aligned and randomly oriented chlorite grains at high angles to S_2 are deformed by spectacular kink bands (Fig. 24b). In addition, several garnet and biotite grains have undergone chlorite alteration (Fig. 7a). Large sericite clusters in the pelitic schist (Fig. 7b) are composed of undeformed grains. Some of these clusters are relatively coarse-grained and contain randomly oriented, recrystallized white mica grains, suggesting growth of white mica during minor retrogression. These microstructural relationships indicate that chlorite and sericite growth occurred during minor retrogression, and kinking must have occurred after growth of the chlorite porphyroblasts.

Microstructures in the Ladron and Capirote plutons suggest low to moderate temperatures during post-D_2 deformation. Monocrystalline quartz ribbons are present in both the white phase of the Ladron pluton and in two qv-mylonites (Fig. 25). Feldspar microstructures in both the main stock and the white phase of the Ladron pluton include fractures, undulatory extinction, deformation twins, subgrains, and recrystallized grains (Fig. 25a). In the qv-mylonites monocrystalline quartz ribbons and relatively large, deformed white mica grains similar to mica fish occasionally exhibit a preferred orientation, possibly indicative of the earliest stages of foliation development (Fig. 25b). Whether or not the micro-structures described in these different units were produced during a single event is unknown. Penetrative fabrics are absent and development of the different structures was heterogeneous.

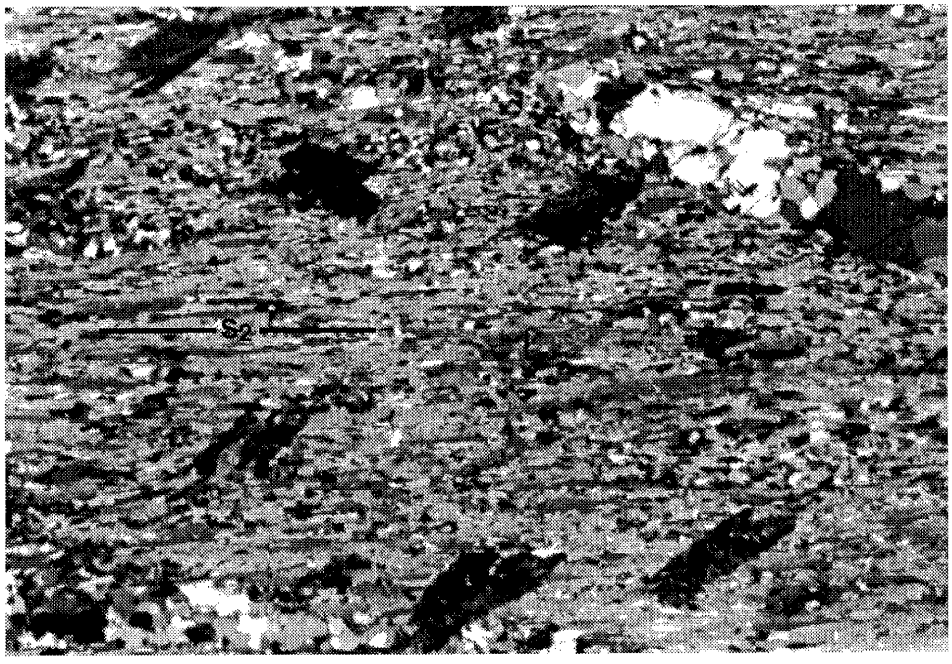

A. Chlorite porphyroblasts (at extinction) are preferentially aligned at a moderate angle to S_2. 8 mm across.

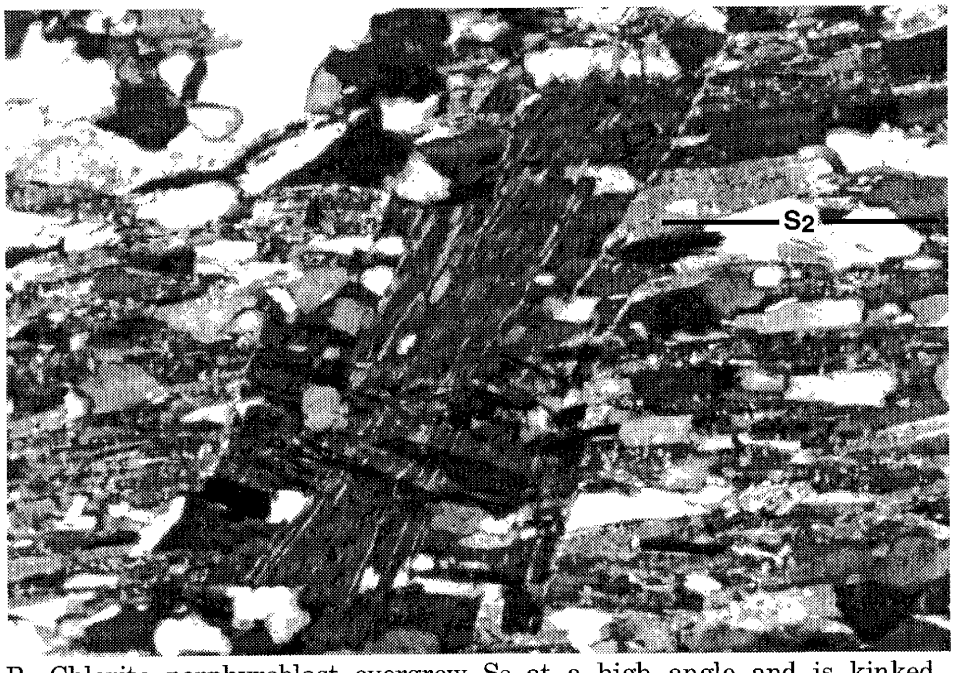

B. Chlorite porphyroblast overgrew S_2 at a high angle and is kinked. 0.8 mm across.

Figure 24. Photomicrographs of pelitic schist cut perpendicular to S_2 and parallel to L_2 showing chlorite porphyroblasts which overgrew the foliation. Crossed polars.

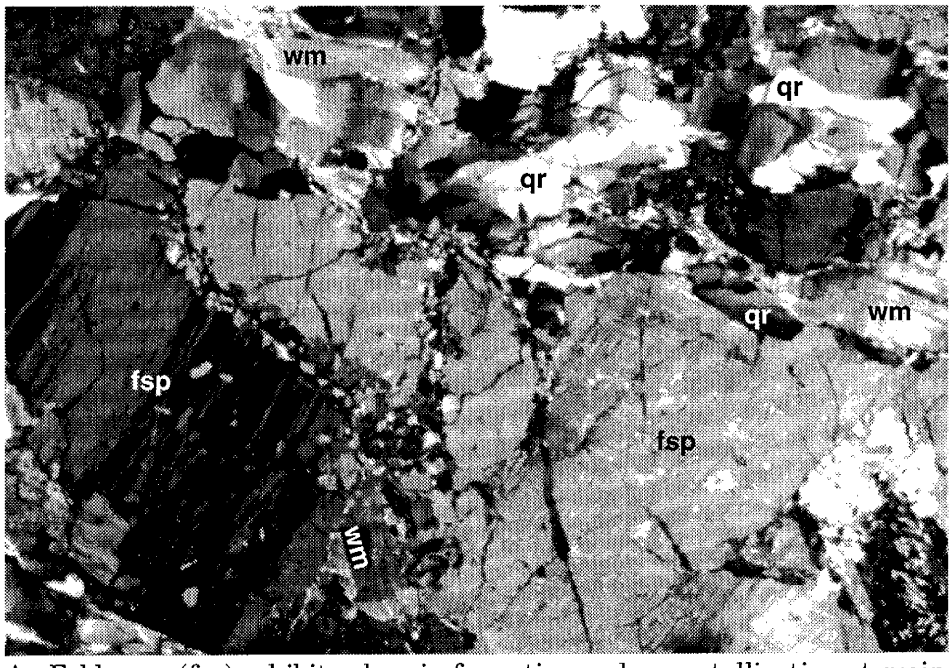

A. Feldspars (fsp) exhibit subgrain formation and recrystallization at grain boundaries and along fractures, and monocrystalline quartz ribbons (qr) and deformed white mica grains (wm) show a preferred alignment.

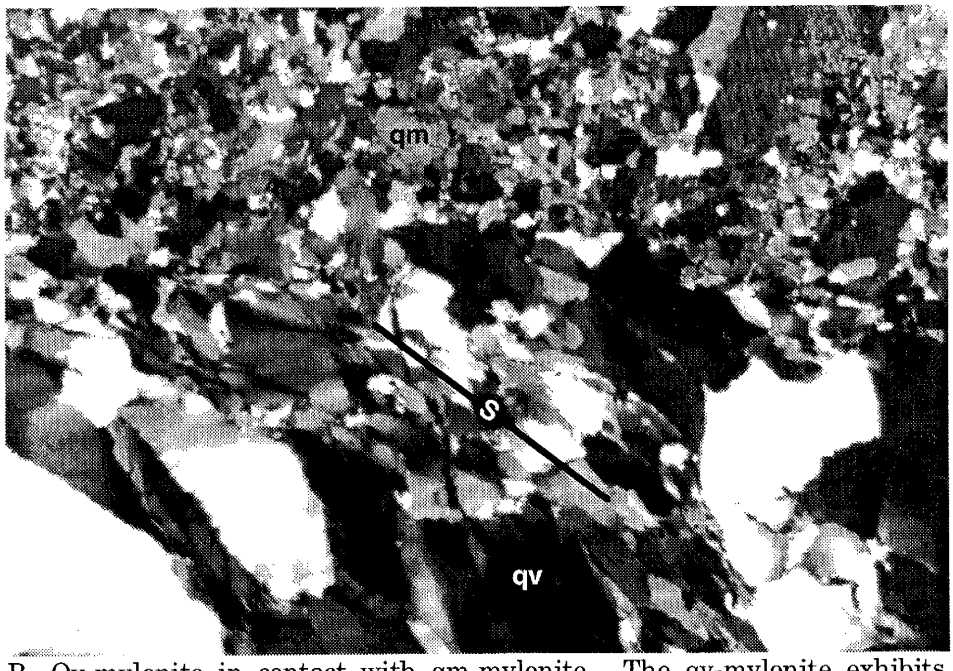

B. Qv-mylonite in contact with qm-mylonite. The qv-mylonite exhibits monocrystalline quartz ribbons, a low temperature microstructure defining an S-surface, which is not evident in the qm-mylonite.

Figure 25. Unoriented photomicrographs of the (A) Ladron and (B) Capirote plutons showing post-D_2 low temperature microstructures. Crossed polars; 8 mm across.

3.1.6 **Crenulation Lineations**

Crenulation lineations (millimeter-scale fold hinges) are found in both S_1 and S_2. Petrographic examination of these lineations indicates that they fold the metamorphic minerals that define these foliations; no mineral growth is associated with the development of the crenulation lineations.

Crenulation lineations in S_1 plunge shallowly to the east (Fig. 26a). The crenulation lineations are roughly parallel to the intersection between S_1 and S_2. These crenulations therefore probably developed during S_2 formation.

Crenulation lineations in S_2 show E-trending concentrations, but vary widely in orientation (Fig. 26b). This may be the result of multiple crenulation-forming events.

3.1.7 **Brittle Deformation**

A few samples from different units show evidence of brittle overprinting. The only map-scale brittle structures observed are fractures within the Ladron pluton, which strike northwest and dip steeply to the southwest (Fig. 4, Plate 1). On a smaller scale, the felsic metavolcanic unit is also locally highly fractured as shown by fracture surfaces crosscutting the S_1 foliation. Shear zones in the Bandit granophyre and meta-arkose locally exhibit well-developed fracture systems oblique to subparallel to S_2. Oxide mineralization has occurred preferentially along these fracture planes. One sample of the quartzofeldspathic biotite schist also exhibits brittle deformation. It contains a 2 mm wide vein of pseudotachylyte which is subparallel to the S_2 foliation but also crosscuts it. The vein contains a few foliated rock fragments with various orientations of S_2.

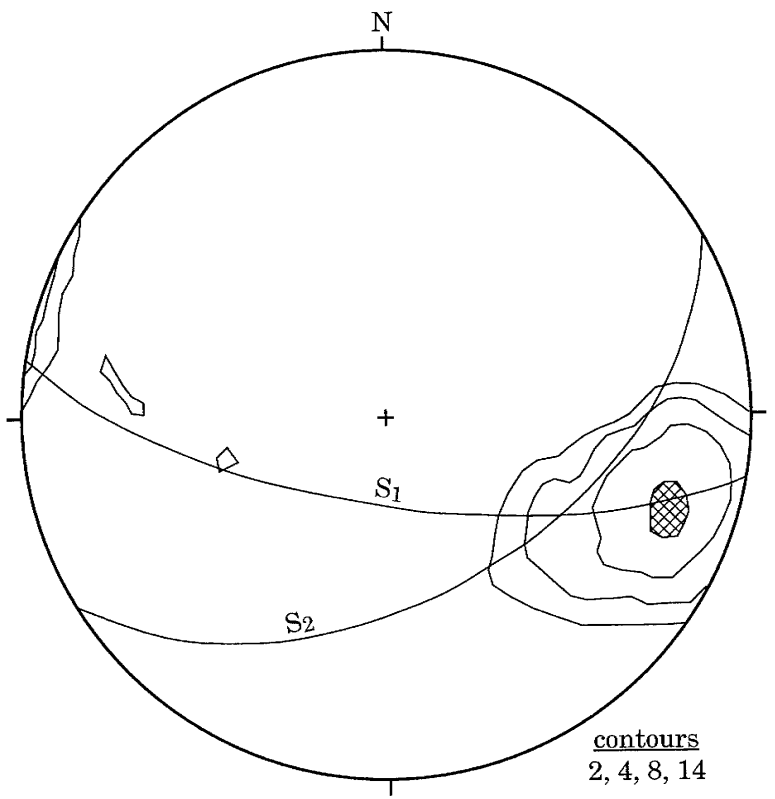

A. Crenulation lineations (n=25) in S_1 and average orientation of S_1 (great circle) in the felsic metavolcanic unit, Bandit granophyre, and meta-arkose. Average orientation of S_2 (great circle) in the Bandit granophyre and meta-arkose.

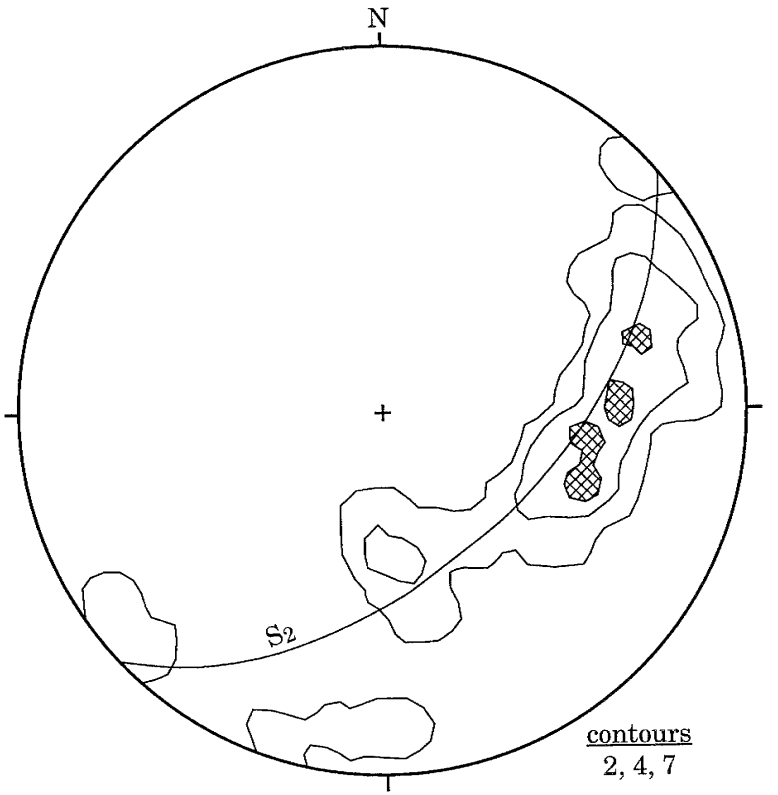

B. Crenulation lineations (n=58) in S2 and average orientation of S2 (great circle) in the Bandit granophyre and the eastern supracrustal sequence.

Figure 26. Lower hemisphere equal area projection of crenulation lineations (contoured) in S_1 and S_2. The area of the diagram below the lowest specified contour is blank; the area above the highest contour is cross-hatched.

3.2 GEOCHRONOLOGY

Samples from the felsic metavolcanic unit, the Bandit granophyre, the Capirote pluton, the Ladron pluton, the white phase of the Ladron pluton, the amphibolite, and nine metaconglomerate granitoid clasts were prepared for U-Pb isotopic dating of zircon and sphene. The presence (and absence) of zircon in the samples is listed in the Appendix; none of these samples were found to contain sphene, although sphene and zircon have been identified petrographically in other localities in the amphibolite unit. Zircon found in felsic igneous rocks is interpreted to have crystallized from a melt and can therefore be used to date crystallization. In contrast, zircon contained in amphibolites is interpreted to have grown during metamorphism because it does not usually crystallize from mafic melts. However, other evidence such as complex crystal morphologies is needed to verify a metamorphic origin (Chamberlain and Bowring, 1990). Sphene contained in amphibolites is generally found to be metamorphic in origin and could also provide an age of metamorphism. However, because of the lower blocking temperature of sphene (500-620°C, Mezger et al., 1991) compared to zircon (>750°C, Ghent et al., 1988), the U-Pb isotopic system of sphene may be reset (frequently due to Pb loss) during subsequent thermal events. If this were the case, the age of the latest thermal event would be dated, rather than the age of mineral growth.

All eleven samples collected for geochronology are listed in the Appendix with sample locations. Each sample was collected to answer specific questions regarding the timing of metamorphism, deformation, and igneous activity (Table 2).

Table 2. Significance of U-Pb isotopic ages.

AGE OF....	SIGNIFICANCE
CRYSTALLIZATION:	(zircon)
Bandit granophyre.....	maximum age of D_1
Capirote pluton.....	maximum age of D_2; minimum age of D_1
Ladron pluton.....	minimum age of D_2; maximum age of post-D_2 events
felsic metavolcanic unit.....	maximum age of D_1
amphibolite.....	igneous zircon: maximum age of D_1; minimum age of eastern metamorphic sequence
granitoid clasts.....	age of plutonic source; maximum age of deposition of metasediments; maximum age of D_1
METAMORPHISM:	
amphibolite.....	metamorphic zircon: minimum age of D_2 sphene: minimum age of D_2 or subsequent thermal event

Dates were obtained for only the felsic metavolcanic unit and the Bandit granophyre, which were sampled in order to constrain the age of the supracrustal rocks and one period of plutonism, respectively. Zircons yielded upper intercept ages of 1658 ± 3 Ma for the felsic metavolcanic unit (Fig. 27a) and 1658 ± 20 Ma for the Bandit granophyre (Fig. 27b) (S.A. Bowring, writ. comm., 1994). These two units are the oldest dated in the Ladron Mountains. The zircons dated are interpreted to yield igneous crystallization ages, which yield maximum age estimates for D_1 since deformation post-dated intrusion of the Bandit granophyre and extrusion of the felsic metavolcanic unit. The close relationship in both time and space (Fig. 4) between these two units suggests that volcanism was closely

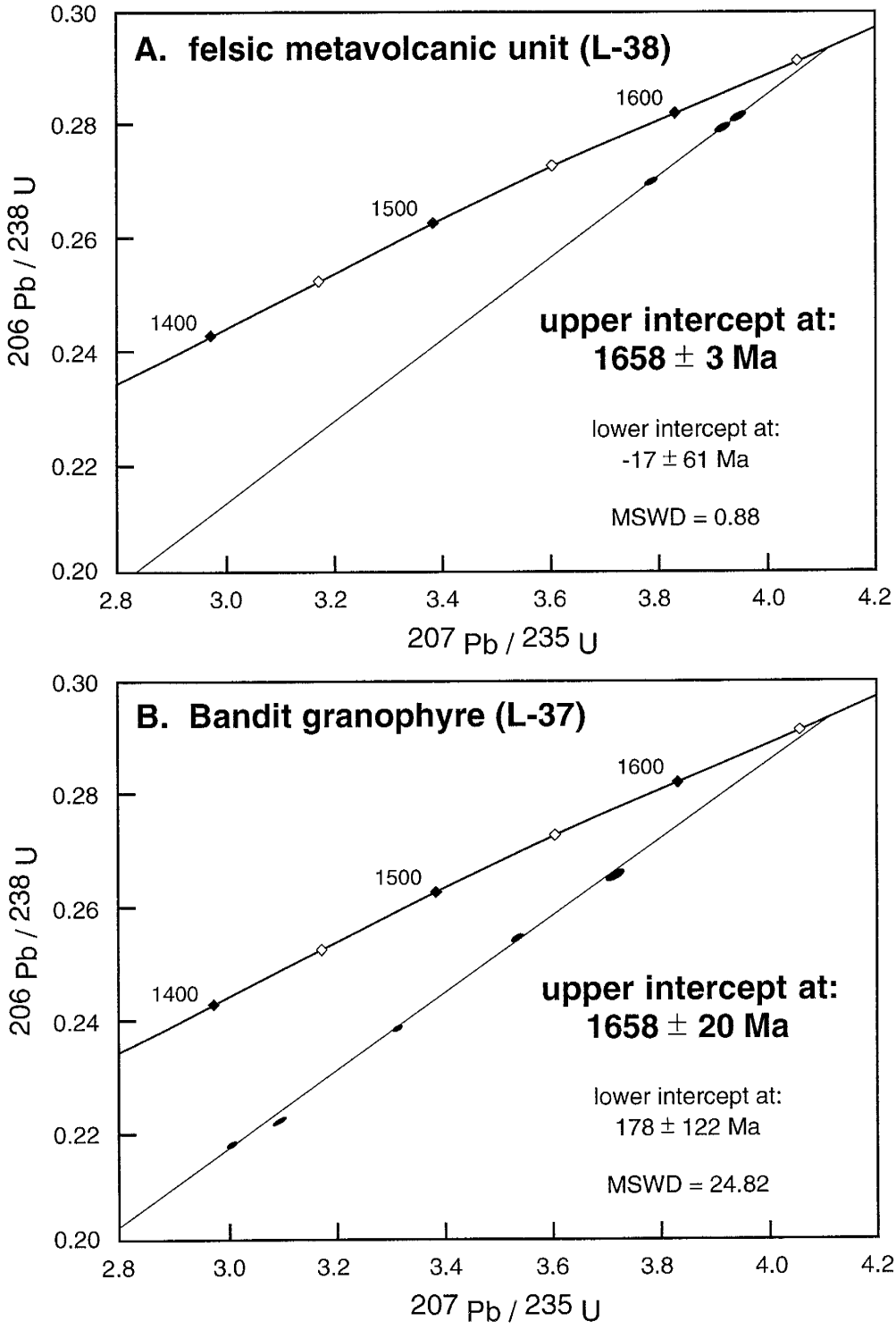

Figure 27. U-Pb concordia diagrams of the A) felsic metavolcanic unit and B) Bandit granophyre. Zircon upper intercept ages are interpreted to represent crystallization ages. MSWD = mean standard weighted deviation.

associated with plutonism at ca. 1.66 Ga, as Condie (1976) first suggested on the basis of geochemical similarity. The ages obtained here are very similar to U-Pb dates on igneous zircon from a metarhyolite (1662 ± 1 Ma) and granite (1655 ± 3 Ma) in the Los Pinos Mountains (Shastri, 1993). Without a true crystallization age on the Capirote pluton it is impossible to say whether this 1.66 Ga igneous event was associated with the Capirote plutonic episode, as Cookro (1978) and Condie (1978) suggested. Nevertheless, the dates are consistent with ages of other moderately to strongly deformed granitoid plutons in New Mexico (Bauer and Pollock, 1993).

Although only zircon from the felsic metavolcanic unit and Bandit granophyre were datable, the significance and importance of obtaining other crystallization ages, metamorphic ages, and depositional ages is discussed below and summarized in Table 2.

Crystallization ages of the granitoid clasts in the metaconglomerate would yield a maximum age limit for deposition, and the age(s) of the plutonic source(s) of the clasts. This would then provide a maximum age for D_1. Crystallization ages of the amphibolites (interpreted as metamorphosed mafic sills or volcanic rocks) would also yield maximum age estimates for D_1 since deformation post-dated intrusion/extrusion of the mafic rocks. A crystallization age for the Capirote pluton would give a minimum age for D_1 because S_1 is not recorded in the pluton. Since D_2 is the earliest recorded event in the Capirote pluton, a crystallization age would provide an upper limit for this event. Also, a date on metamorphic sphene in the amphibolites would give a minimum age for D_2. Likewise, the age of crystallization of the Ladron pluton would constrain the minimum age of D_2 and maximum age of post-D_2 events because the Ladron pluton was emplaced post-D_2.

Another approach to obtain the age of metamorphism associated with D_2 would be to use $^{40}Ar/^{39}Ar$ dating of amphibole known to have grown in the amphibolite during D_2. However, post-D_2 thermal events could have reset the Ar-Ar isotopic systematics, and such dates would have to be highly scrutinized; would they represent the age of D_2 metamorphism or the age of subsequent thermal events?

3.3 RELATIVE TIMING OF EVENTS

3.3.1 **Metamorphism and Deformation**

A summary of the character and timing of metamorphism and deformation in the Ladron Mountains is included in Table 3. Because S_1 is only well-preserved in rocks without metamorphic index minerals, the relative timing of deformation and metamorphism is difficult to constrain. By using microstructural observations, however, metamorphic conditions during deformation have been estimated. As discussed earlier, microstructures within the granophyre, meta-arkose, and felsic metavolcanic units suggest that amphibolite facies conditions accompanied D_1. D_2 was accompanied by growth of metamorphic index minerals in the pelitic schist (Table 3). Thus, porphyroblast/matrix relationships were used to determine the relative timing of D_2 deformation and metamorphism. As previously discussed, peak metamorphic conditions (amphibolite grade) outlasted deformation. Post-D_2 local retrogression has also been noted.

Table 3. Relative timing of deformation and metamorphism.

	D_1			D_2			post-D_2 events
Deformation Stage	pre	syn	post	pre	syn	post	
Mineral Growth:							retrogression
white mica		xxx			xxx xxx		x
biotite		xxx			xxx	xxxxxxxx	
garnet		?	xxxx		xxx	xxx	
staurolite						xxx	
amphibole		xxx			xxx	xxxxxxxx	
chlorite							x
sericite							x
Metamorphic Grade		amphibolite facies			amphibolite facies		low-moderate temperatures
S Formed		S_1			S_2		none observed
S Folded					S_1		S_2
Shear Sense		dextral strike-slip on EW shear planes			normal-oblique, SE-side-down		none observed

3.3.2 **Metamorphism and Intrusion**

Noble (1950), Black (1964), Haederle (1966), Condie (1976), and Taylor (1986) previously asserted that contact metamorphic features are absent adjacent to both the Ladron and Capirote intrusions. The lack of observable contact aureoles around either of the plutons prevents interpretation regarding metamorphism associated with pluton emplacement. Nevertheless, two observations can be made with regard to the apparent lack of a contact aureole adjacent to the Capirote pluton: (1) it may have been erased by D_2 metamorphism; and/or (2) the wall rocks were too hot to be overprinted by an aureole during intrusion. That is, they were at a similar temperature to that of the pluton during intrusion, which could have resulted from either deep emplacement of the pluton or synchronous regional metamorphism. Because only minor metamorphism post-dated intrusion of the Ladron pluton, the apparent absence of a contact aureole must be due to a relatively small difference in temperature between the wall rocks and the pluton.

3.3.3 **Intrusion and Deformation**

Criteria used to recognize syn-deformational intrusion include the following: (1) the continuity of foliations and stretching lineations within and outside the pluton (Brun and Pons, 1981); (2) foliation triple points in country rock near the ends of the pluton (Ledru and Brun, 1977); (3) decreasing gradation from higher-grade contact metamorphic assemblages into regional metamorphic assemblages moving away from the pluton margins (Paterson and Tobisch, 1988); (4) gradation from a magmatic foliation within the pluton to a parallel tectonic foliation in the country rock (Paterson et al., 1989); and (5) the general agreement of pluton shapes with regional structures (Brun and Pons, 1981). In order to verify syn-deformational intrusion, a combination of these criteria are needed. Only (1) is evident in the Bandit granophyre and Capirote pluton which exhibit some continuity of S_1/L_1 and S_2/L_2, respectively, within and outside of the plutons as shown in Plate 1. However, because these structures within the plutons are strongly localized, this reflects solid-state deformation (tectonic foliations) and not magmatic foliations (Paterson et al., 1989).

Although contact metamorphic features are absent, a few important observations have been with respect to the timing of deformation and intrusion. The Capirote pluton is macroscopically deformed with D_2 fabrics locally developed. Because the pluton does not record S_1, it must have been emplaced subsequent to D_1. The Bandit granophyre does record D_1, so it may be unrelated to the Capirote pluton. Alternatively, the Bandit granophyre could have been an early phase and the Capirote pluton a later phase of the same intrusion, in which case they would bracket D_1 in time.

The Ladron pluton, in contrast, is macroscopically undeformed, but locally shows evidence of strain at the microscopic scale. The low temperature character of these post-D_2 fabrics indicates that the Ladron pluton crystallized and cooled significantly prior to their formation. That is, the deformation was not synchronous with emplacement/cooling of the Ladron pluton because of the locally high temperatures associated with intrusion. Thus minor deformation post-dated the 1.3(?) Ga plutonic event.

4. DISCUSSION

NE-striking foliations are the dominate structures in nearby exposures of Proterozoic rocks including the Magdalena Mountains (Bauer and Williams, 1994), Lemitar Mountains (McLemore, 1980), Manzano Mountains (Bauer et al., 1993), and Los Pinos Mountains (Shastri, 1993) (Fig. 1). In the latter two, this foliation (S_2) has overprinted an older foliation (S_1). Williams (1991) and Bauer (1993) proposed that S_1 and S_2 formed during a single, progressive deformational event in the Tusas and Picuris Mountains, respectively (Fig. 1). Recent work in the Manzano Mountains suggests that S_2 is a composite foliation, initially developed at ca. 1.6 Ga and reactivated during intrusion of the Priest pluton at ca. 1.4 Ga (Karlstrom and Grambling, 1993; Thompson and Karlstrom, 1993). Amphibolite facies metamorphism accompanied both D_1 and D_2 in these areas, and often outlasted deformation. Structures which record top-to-the-south shear along S_2 are found in the following areas: the Tusas Range (Williams, 1991), the Taos Range (Grambling et al., 1989), the Picuris Range (Bauer, 1993), the Cimarron Range (Grambling and Dallmeyer, 1990), the Manzano Mountains (Thompson et al., 1991), and the Zuni Mountains (Mawer and Bauer, 1989).

Although the Ladron Mountains have a complex metamorphic and deformational history, there is sufficient information available to evaluate the relative timing of events. This area preserves S_1, which is only partially preserved in most other ranges in New Mexico.

Based on the comparison between orientation and shear sense for S_1 and S_2 (Table 2), it appears that two different deformational regimes were operating at different times. There is no evidence to suggest that the change from one regime to the other was progressive except for the similarity in metamorphic grade. The similarity in metamorphic grade during D_2 and the character of fabrics preserved within 1.6 and 1.4 Ga plutons in both the Ladron Mountains and the Manzano Mountains suggests that the two mountain ranges record the same metamorphic and deformational history. Whether S_2 in the Ladron Mountains was reactivated during intrusion of the Ladron pluton, as S_2 was during intrusion of the Priest pluton in the Manzano Mountains, is still uncertain because of the absence of a contact aureole.

Now that field-based structural studies have determined the relative timing of plutonism and deformation, an absolute age of intrusion on the Capirote pluton would tightly constrain the ages of D_1 and D_2. The major deformation as recorded by the NE-striking foliation in the Magdalena Mountains has been reliably dated at 1664-1654 Ma (Bauer and Williams, 1994). If this foliation correlates with S_2 elsewhere in New Mexico, D_2 in the Ladron Mountains may be similar in age to the deformational event recorded in the Magdalena Mountains. Thus, it is possible that D_1 and D_2 in the Ladron Mountains are closely spaced in time, and that the Bandit granophyre and Capirote pluton may be pulses of a single intrusive event.

The lack of constraints on the absolute age of intrusion of the Ladron pluton makes correlations with other young plutons equivocal. The 1.3 Ga whole rock Rb-Sr date (White, 1977) on the Ladron pluton may reflect a true crystallization age because deformation is minimal and no evidence for metamorphism was observed. Thus, the Ladron pluton probably corresponds to the widespread 1.35-1.45 Ga plutonic event documented throughout the Southwest (Grambling, 1986; Grambling et al., 1989). A later thermal event at 1.14 Ga may be recorded by the whole rock Rb-Sr date on the felsic metavolcanic (White, 1977), but this is speculative.

Data from this study support the view, based on the weakly deformed 1.3 Ga Ladron pluton, that major deformation and metamorphism recorded within Proterozoic rocks occurred prior to 1.3 Ga. Although the moderately deformed Capirote pluton is not constrained to be ca. 1.6 Ga in age, this age would be consistent with other more strongly deformed, ca. 1.6 Ga plutons in New Mexico.

5. CONCLUSIONS

5.1 SUMMARY

Relative timing of plutonism, deformation, and metamorphism can be difficult to resolve in areas that have undergone a single tectonic episode (Paterson and Tobisch, 1988). In areas that are multiply deformed and metamorphosed, these relationships are further complicated. Although absolute dates on intrusional, deformational, and metamorphic events in the Ladron Mountains are few, a relative sequence of Proterozoic events can be determined (Fig. 28).

1. The Bandit granophyre and felsic metavolcanic unit were permissively produced in the same igneous event at ca. 1.66 Ga (U-Pb dates on zircon), coincident in time with several plutonic and metavolcanic rocks in central and northern New Mexico (Bauer and Pollock, 1993) and in Arizona (Karlstrom and Bowring, 1991) during the Mazatzal Orogeny.
2. The earliest deformational event (D_1) for which evidence is preserved produced a foliation, S_1, in the Bandit granophyre, felsic metavolcanic unit, and supracrustal sequence. D_1 is characterized by dextral strike-slip movement on WNW-oriented shear surfaces accompanied by amphibolite facies metamorphism.
3. Intrusion of the Capirote pluton occurred subsequent to D_1 and prior to D_2. Both deformational episodes possibly occurred during a single orogenic event, the Mazatzal Orogeny.
4. D_2 resulted in overprinting of D_1 fabrics and produced the dominant NE-striking foliation in the metasedimentary and metamorphic sequences, which is correlative with structures produced throughout New Mexico and during the Mazatzal Orogeny in Arizona. S_2 development was spatially heterogeneous. SE-side-down, oblique-

normal movement and amphibolite facies metamorphism characterize D_2. Metamorphism outlasted D_2.

5. Post-D_2 emplacement of the Ladron pluton occurred at approximately 1.3-1.4 Ga, perhaps as part of the major thermal event in New Mexico at this time.
6. Later deformation of unknown age includes heterogeneously developed, low temperature structures in the pelitic schist and in the Capirote and Ladron plutons. Brittle deformation structures (fractures, pseudotachylyte) observed in several units overprint all other features.

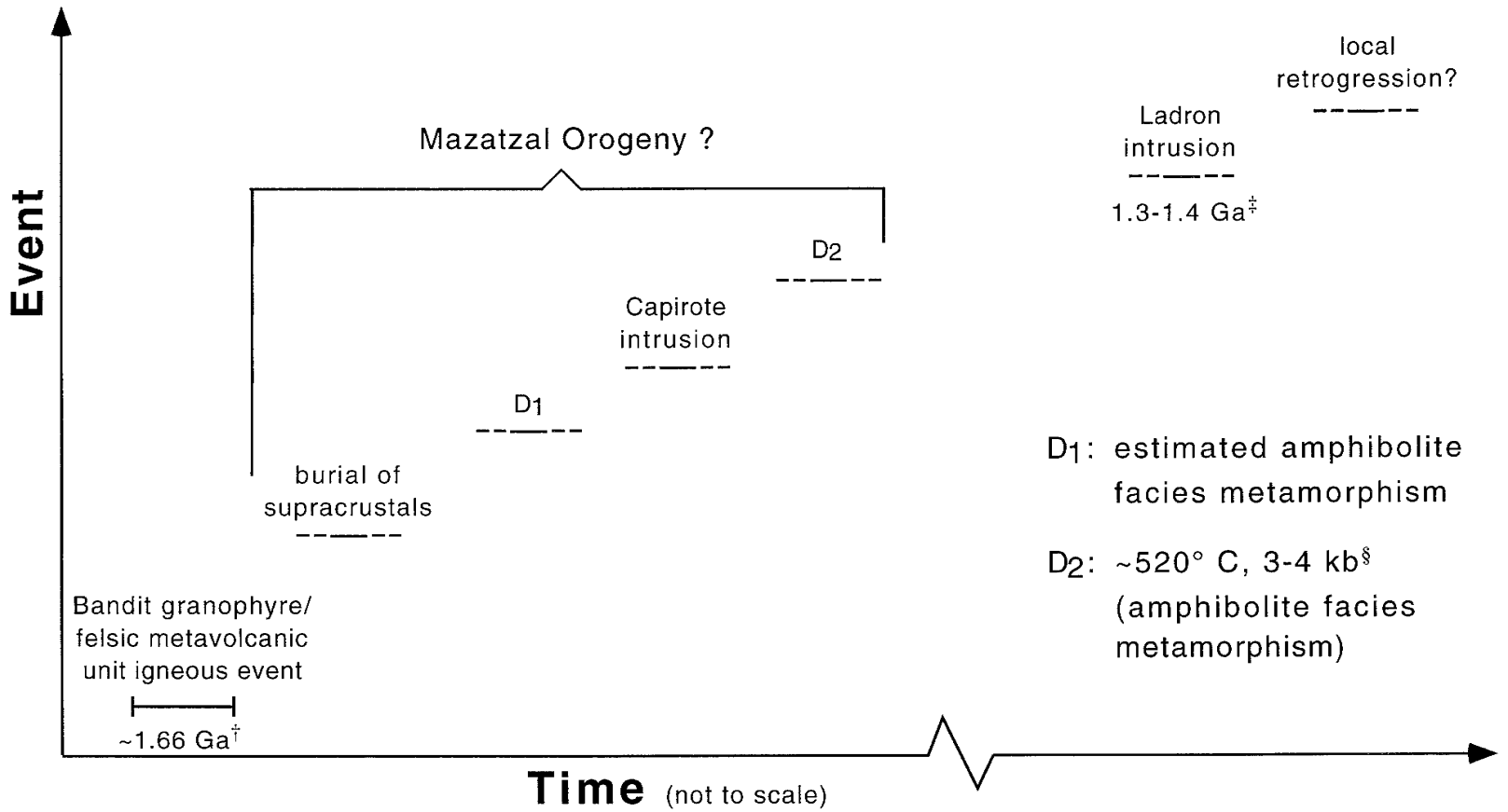

Figure 28. Relative timing of intrusion, deformation, and metamorphism. §P-T data from Taylor (1986); †1658 ± 20 Ma and 1658 ± 3 Ma U-Pb dates on zircon from Bowring (1994, written comm.); ‡1291 ± 51 Ma Rb-Sr whole rock date from White (1977).

5.2 IMPLICATIONS

D_1 and D_2 may have been distinct, unrelated deformational events, or they may have been related to a single orogenic event. Deformation can vary dramatically in space and time within orogenic belts. For example, dextral and sinistral strike-slip motion, thrusting, and normal movement all participated in formation of the Himalayas as we see them today (Molnar and Tapponier, 1975; Burchfiel et al., 1992). Furthermore, Karlstrom and Williams (in review) have suggested that transpressional convergence caused partitioning of strain into both dip-slip and strike-slip components during accretion of Proterozoic arcs in central Arizona. Thus, the deformational history of the Ladron Mountains is compatible with models of accretion at 1.75-1.65 Ga in the southwestern United States (Bowring and Karlstrom, 1990; Bauer and Williams, 1994).

5.3 FUTURE STUDIES

Clearly, additional geochronologic data are needed for a complete understanding of the timing of intrusion, metamorphism, and deformation in the Ladron Mountains. U-Pb zircon dates on the Capirote and Ladron plutons and granitoid clasts would: 1) determine whether the plutons are ca. 1.6 or 1.4 Ga plutons; 2) constrain the ages of D_1 and D_2; and 3) provide a maximum age for deposition of the clastic metasedimentary sequence. U-Pb dating of metamorphic sphene in the amphibolite could constrain the age of metamorphism coincident with D_2. In addition, rare-earth element geochemistry on the granitoid clasts might provide insight into the source rock, and hence the origin of the metasediments. Such additional research would allow a more comprehensive evaluation and comparison with other Proterozoic rocks in New Mexico, which could further constrain the timing and character of Proterozoic metamorphic and deformational events in the southwestern United States.

APPENDIX. Locations of U-Pb geochronology samples in the Ladron Mountains.

SAMPLE NUMBER‡	LITHOLOGY	latitude (N)	longitude (W)	utm coordinates m(N), m(E)
L-4 (NM-62a)†	metaconglomerate granitoid clast	34°25'16"	107°03'50"	3810590, 310320
L-6 (NM-62b)†	metaconglomerate granitoid clast	34°25'23"	107°03'53"	3810800, 310280
L-7 (NM-62c)†	metaconglomerate granitoid clast	34°25'23"	107°03'53"	3810800, 310280
L-16 (NM-62d)†	metaconglomerate granitoid clast	34°25'23"	107°03'53"	3810800, 310280
L-20 (NM-60b)†§	white phase Ladron quartz monzonite	34°25'05"	107°03'23"	3810250, 311050
L-21 (NM-60a)†§	Ladron quartz monzonite (LQM)	34°25'10"	107°03'10"	3810390, 311350
L-22 (NM-61)†§	Capirote quartz monzonite (CQM)	34°25'20"	107°02'20"	3810670, 312630
L-37 (NM-64)	Bandit granophyre (1658 ± 20 Ma)	34°25'41"	107°04'30"	3811350, 309330
L-38 (NM-63)	felsic metavolcanic unit (1658 ± 3 Ma)	34°25'32"	107°04'35"	3811080, 309200
L-70 (NM-67)†§	amphibolite	34°25'07"	107°03'32"	3810280, 310800
L-105 (NM-74)†	undeformed pegmatite (of LQM) in CQM	34°24'40"	107°03'27"	3809500, 310900

‡New Mexico geochronology sample numbers in parentheses
† samples with no zircon
§ zircon identified in thin section from other sample localities in the unit

REFERENCES

Bauer, P.W. and Pollock, T.R., 1993. Compilation of Precambrian isotopic ages in New Mexico. *New Mexico Bureau of Mines and Mineral Resources, Open-File Report 389, 139p.*

Bauer, P.W., Karlstrom, K.E., Bowring, S.A., Smith, A.G., and Goodwin, L.B., 1993. Proterozoic plutonism and regional deformation: New constraints from the southern Manzano Mountains, central New Mexico. *New Mexico Geology, v.14, no. 3:* **49-55**.

Bauer, P.W. and Williams, M.L., 1994. The age of Proterozoic orogenesis in New Mexico, U.S.A. *Precambrian Research (in press).*

Bauer, P.W., 1993. Proterozoic tectonic evolution of the Picuris Mountains, northern New Mexico. *Journal of Geology, 101:* **483-500**.

Bell, D.A., 1985. Structural and age relationships in the Embudo granites, Picuris Mountains, New Mexico. *M.S. Thesis, University of Texas, Dallas, 175 p.*

Bell, T.H. and Rubenach, M.J., 1983. Sequential porphyroblast growth and crenulation cleavage development during progressive deformation. *Tectonophysics, 92:* **171-194**

Berthé, D., Choukroune, P., and Jegouzo, P., 1979a. Orthogneiss, mylonite and non-coaxial deformation of granites: the example of the south Amoricain shear zone. *Journal of Structural Geology, 1:* **31-42**.

Black, B.A., 1964. The geology of the northern and eastern parts of the Ladron Mountains, Socorro County, New Mexico. *M.S. Thesis, University of New Mexico, Albuquerque, 117 p.*

Boullier, A-M. and Bouchez, J-L., 1978. Le quartz en rubans dans les mylonites. *Bull. Soc. Geol. Fr., 7:* **253-262**.

Bowring, S.A. and Condie, K.C., 1982. U-Pb zircon ages from northern and central New Mexico. *Geological Society of America, Abstracts with Programs, 8:* **304**.

Bowring, S.A., Kent, S.C., and Sumner, W., 1983. Geology and U-Pb geochronology of Proterozoic rocks in the vicinity of Socorro, New Mexico. *New Mexico Geological Society, Guidebook 34:* **137-142**

Bowring, S.A. and Karlstrom, K.E., 1990. Growth, stabilization, and reactivation of Proterozoic lithosphere in the southwestern United States. *Geology, 18:* **1203-1206**.

Brookins, D.G. and Majumdar, A., 1982. The Sandia Granite, New Mexico-Biotite metamorphic and whole rock Rb-Sr ages. *Isochron / West, 12:* **9**.

Brun, J.P. and Pons, J., 1981. Strain patterns of pluton emplacement in a crust undergoing non-coaxial deformation, Sierra Morena, Southern Spain. *Journal of Structural Geology, 3:* **219-229**.

Burchfiel, B.C., Chen, Z., Hodges, K.V., Liu, Y., Royden, L.H., Deng, C., and Xu, J., 1992. The south Tibetan detachment system, Himalayan Orogen: Extension contemporaneous with and parallel to shortening in a collisional mountain belt. *Geological Society of America, Special Paper 269, 41 p.*

Chamberlain, K.R. and Bowring, S.A., 1990. U-Pb geochronology of Proterozoic rocks in northwestern Arizona: Implications for crustal growth. *Journal of Geology, 98:* **399-416**.

Condie, K.C., 1976. Precambrian rocks of Ladron Mountains, Socorro County, New Mexico. *New Mexico Bureau of Mines and Mineral Resources, Geologic Map 38.*

Condie, K.C., 1978. Geochemistry of Proterozoic granitic plutons from New Mexico, U.S.A. *Chemical Geology, 21:* **131-149**.

Condie, K.C. and Budding, A.J., 1979. Geology and geochemistry of Precambrian rocks, central and south-central New Mexico. *New Mexico Bureau of Mines and Mineral Resources, Memoir 35, 58 p.*

Condie, K.C., 1982. Plate tectonics model for Proterozoic continental accretion in the southwestern United States. *Geology, 10:* **37-42**.

Condie, K.C., 1986. Geochemistry and tectonic setting of Early Proterozoic supracrustal rocks in the southwestern United States. *Journal of Geology, 94:* **845-864**.

Condie, K.C., Bickford, M.E., and Van Schmus, W.R., 1987. Accretion and tectonic evolution of North America 1600-1800 Ma ago. *Geological Association of Canada, Programs Abstracts, 22:* **113**.

Cookro, T.M., 1978. Petrology of Precambrian granitic rocks of the Ladron Mountains, Socorro County, New Mexico. *M.S. Thesis, New Mexico Institute of Mining and Technology, Socorro, 66 pp.*

Dallmeyer, R.D., Grambling, J.A., and Thompson, A.G., 1990. Age and character of Proterozoic polymetamorphism in New Mexico. *Geological Society of America, Abstracts with Programs, 22:* **113**.

Debat, P., Soula, J.C., Kubin, L., and Vidal, J.L., 1978. Optical studies of natural deformation microstructures in feldspars (gneisses and pegmatites from Occitanie, southern France. *Lithos, 11:* **133-146**.

Farquhar, P., 1976. Petrology and geochemistry of the Precambrian metavolcanics of Ladron Mountain, New Mexico. I*ndependent Study, New Mexico Institute of Mining and Technology, Socorro, 45 p.*

Gapais, D., 1989. Shear structures within deformed granites: Mechanical and thermal indicators. *Geology, 17:* **1144-1147**

Gapais, D. and White, S.H., 1982. Ductile shear bands in naturally deformed quartzite. *Textures and Microstructures, 5:* **1-17**.

Ghent, E.D., Stout, M.Z., and Parrish, R.R., 1988. Determination of metamorphic pressure-temperature-time (PTt) paths. *Short Course on Heat, Metamorphism, and Tectonics, Mineralogical Association of Canada:* **155-188**.

Goodwin, L.B. and Wenk, R.H., 1990. Intracrystalline folding and cataclasis in biotite of the Santa Rosa mylonite zone: HVEM and TEM observations. *Tectonophysics, 172:* **201-214**.

Goodwin, L.B., Ralser, S., Bauer, P.W., and Karlstrom, K.E., 1992. Mylonitization events bracketing a granitoid intrusion-a Proterozoic example from the Manzano Mountains, New Mexico. *Geological Society of America, Abstracts with Programs, v. 24, no.7:* **146**.

Grambling, J.A., 1986. Crustal thickening during Proterozoic metamorphism and deformation in New Mexico. *Geology, 14:* **149-152**.

Grambling, J.A., Williams, M.L., Smith, R.F., and Mawer, C.K., 1989. The role of crustal extension in the metamorphism of Proterozoic rocks in New Mexico. *Geological Society of America, Special Paper 235:* **87-110**.

Grambling, J.A. and Dallmeyer, R.D., 1990. Proterozoic tectonic evolution of the Cimarron Mountains, north-central New Mexico. *New Mexico Geological Society, Guidebook 41:* **161-170**.

Grambling, J.A. and Dallmeyer, R.D., 1993. Tectonic evolution of Proterozoic rocks in the Cimarron Mountains, northern New Mexico, U.S.A. *Journal of Metamorphic Geology, 11:* **739-755**.

Grambling, J.A. and Thompson, A.G., 1992. Middle Proterozoic thrusting in central New Mexico. *Geological Society of America, Abstracts with Programs, v. 24, no.7:* **92**.

Haederle, W.F., 1966. Structure and metamorphism in the southern Sierra Ladrons, Socorro County, New Mexico. *M.S. Thesis, New Mexico Institute of Mining and Technology, Socorro, 56 pp*.

Holdaway, M.J., 1971. Stability of andalusite and the aluminum silicate phase diagram. *American Journal of Science, 271:* **97-131**.

Karlstrom, K.E. and Bowring, S.A., 1988. Early Proterozoic assembly of tectonostratigraphic terranes in southwestern North America. *Journal of Geology, 96:* **561-576**.

Karlstrom, K.E. and Bowring, S.A., 1991. Styles and timing of Early Proterozoic deformation in Arizona: Constraints on tectonic models. *Arizona Geological Society Digest, 19:* **181-192**.

Karlstrom, K.E. and Grambling, J.A., 1993. Proterozoic orogenic history in New Mexico; a merging of conflicting models. *New Mexico Geological Society Proceedings Volume:* **16**.

Karlstrom, K.E. and Williams, M.L., 1994. The case for simultaneous deformation, metamorphism, and plutonism: An example from Proterozoic rocks in central Arizona. *Journal of Structural Geology (in review)*.

Ledru, P. and Brun, J.P., 1977. Utilisation des fronts et des trajectoires de schistosité dans l'étude des relations entre tectonique et intrusion granitique: exemple du granite de Flamanville (Manche). *Séanc. Acad. Sci., Paris, 258:* **1199-1202**.

Lister, G.S. and Snoke, A.W., 1984. S-C mylonites. *Journal of Structural Geology, 6:* **617-638**.

Mawer, C.K. and Bauer, P.W., 1989. Precambrian rocks of the Zuni uplift: a summary, with new data on ductile shearing. *New Mexico Geological Society, Guidebook 40:* **143-148**.

McLemore, V.T., 1980. Geology of the Precambrian rocks of the Lemitar Mountains, Socorro County, New Mexico. *New Mexico Bureau of Mines and Mineral Resources, Open-File Report 122, 207 p.*

Mezger, K., Rawnsley, S.R., Bohlen, S.R., and Hanson, G.N., 1991. U-Pb garnet, sphene, monazite, and rutile ages: Implications for the duration of high-grade metamorphism and cooling histories, Adirondack Mts., New York. *Journal of Geology, 99:* **415-428**.

Molnar, P. and Tapponnier, P., 1975. Cenozoic tectonics of Asia: Effects of a continental collision. *Science, 189:* **419-426**.

Noble, E.A., 1950. Geology of the southern Ladron Mountains, Socorro County, New Mexico. *M.S. Thesis, University of New Mexico, Albuquerque, 156 pp.*

Paterson, S.R. and Tobisch, O.T., 1988. Using pluton ages to date regional deformations: problems with commonly used criteria. *Geology, 16:* **1108-1111**.

Paterson, S.R., Vernon, R.H., and Tobisch, O.T., 1989. A review of the criteria for the identification of magmatic and tectonic foliations in granitoids. *Journal of Structural Geology, 11:* **349-363**.

Ramsay, J.G., 1980. Shear zone geometry: a review. *Journal of Structural Geology, 2:* **83-100**.

Reed, J.C., Bickford, M.E., Premo, W.R., Aleinikoff, J.N., and Pallister, J.S., 1987. Evolution of the Early Proterozoic Colorado province: constraints from U-Pb geochronology. *Geology, 15:* **861-865**.

Shastri, L.L., 1993. Proterozoic geology of the Los Pinos Mountains, central New Mexico: Timing of plutonism, deformation and meta-morphism. *M.S. Thesis, University of New Mexico, Albuquerque, 82 pp*.

Simpson, C., 1985. Deformation of granitic rocks across the brittle-ductile transition. *Journal of Structural Geology, 7:* **503-511**.

Starkey, J., 1970. A computer programme to prepare orientation diagrams. In: *Experimental and Natural Rock Deformation, Paulitsch, P., ed., Springer Publishers:* **51-74**.

Starkey, J., 1977. The contouring of orientation data represented in spherical projection. *Canadian Journal of Earth Science, 14:* **268-277**.

Taylor, K.R., 1986. Structural and stratigraphic analysis of Precambrian rocks, south-central Ladron Mountains, Socorro County, New Mexico. *M.S. Thesis, University of New Mexico, Albuquerque, 156 pp.*

Thompson, A.G., Grambling, J.A., and Dallmeyer, D.R., 1991. Proterozoic tectonic history of the Manzano Mountains, central New Mexico. *New Mexico Bureau of Mines and Mineral Resources, Bulletin 137:* **71-77**.

Thompson, A.G. and Karlstrom, K.E., 1993. Porphyroblast-matrix relationships used to recognize polyphase geologic history in middle Proterozoic rocks of central New Mexico. *New Mexico Geological Society Proceedings Volume:* **18**.

Turner, F.J., 1981. *Metamorphic Petrology: Mineralogical, Field, and Tectonic Aspects*. Hemisphere Publishing Corporation, Washington, 524 p.

White, D.L., 1977. A Rb-Sr isotopic geochronologic study of Precambrian intrusives of south-central New Mexico. *Ph.D. Thesis, Miami University, Oxford, Ohio, 88 pp.*

Williams, M.L., 1990. Proterozoic geology of northern New Mexico: Recent advances and ongoing questions. *New Mexico Geological Society, Guidebook 41:* **151-159**.

Williams, M.L., 1991. Heterogeneous deformation in a ductile fold-thrust belt: The Proterozoic structural history of the Tusas Mountains, New Mexico. *Geological Society of America, Bulletin 103:* **171-188**.

This document is accepted on behalf of the faculty of the Institute by the following committee:

Adviser

November 12, 1994
Date

I release this document to New Mexico Institute of Mining and Technology.

Students Signature

12-8-94
Date